SANDIA REPORT
SAND2001-1187
Unlimited Release
Printed April 2001

Investigation of Mass Distribution in a Stabilized Plume for Various Lofting Energies and Meteorological Conditions

Julie J. Gregory and Frederick T. Harper

Prepared by
Sandia National Laboratories
Albuquerque, New Mexico 87185 and Livermore, California 94550

Sandia is a multiprogram laboratory operated by Sandia Corporation, a Lockheed Martin Company, for the United States Department of Energy under Contract DE-AC04-94AL85000.

Issued by Sandia National Laboratories, operated for the United States Department of Energy by Sandia Corporation.

Available to DOE and DOE contractors from
U.S. Department of Energy
Office of Scientific and Technical Information
P.O. Box 62
Oak Ridge, TN 37831

Telephone: (865)576-8401
Facsimile: (865)576-5728
E-Mail: reports@adonis.osti.gov
Online ordering: http://www.doe.gov/bridge

Available to the public from
U.S. Department of Commerce
National Technical Information Service
5285 Port Royal Rd
Springfield, VA 22161

Telephone: (800)553-6847
Facsimile: (703)605-6900
E-Mail: orders@ntis.fedworld.gov
Online order: http://www.ntis.gov/ordering.htm

SAND2001-1187
Unlimited Release
Printed April 2001

Investigation of Mass Distributions in a Stabilized Plume for Various Lofting Energies and Meteorological Conditions

Julie J. Gregory
Mission Analysis and Simulation Department

Frederick T. Harper
High Consequence Assessment and Technology Department

Sandia National Laboratories
P.O. Box 5800
Albuquerque, NM 87185-0977

Abstract

In support of the Cassini Mission Final Safety Analysis Report (FSAR), Sandia National Laboratories (SNL) was requested by Lockheed Martin Corporation (LMC) to investigate for various scenarios, the distribution of aerosol and particulate mass in a stabilized buoyant plume created as a result of a fireball explosion. The information obtained from these calculations is to provide background information for the radiological consequence analysis of the FSAR. Specifically, the information is used to investigate the mass distribution within the "cap and stem" portions of the initial fireball plume, a modeling feature included in the SATRAP module in the LMC SPARRC code. The investigation includes variation of the plume energy and the application of several meteorological conditions for a total of seven sensitivity case studies. For each of the case studies, the calculations were performed for two configurations of particle mass in the plume (total mass and plutonium mass).

This page intentionally left blank.

Acknowledgments

The authors would like to acknowledge Nelson Deane and Chuong Ha of Lockheed Martin Corporation for their steadfast support, inspiration, and technical guidance for this work. We would also like to acknowledge the sponsorship of Earl Wahlquist of the U.S. Department of Energy. In addition, we appreciate the technical leadership that Vince Dandini of Sandia National Laboratories has brought to bear upon this study.

Table of Contents

List of Figures

List of Tables

1.0 Executive Summary

In support of the Cassini Mission Final Safety Analysis Report (FSAR) [LMC, 1996], Sandia National Laboratories (SNL) was requested by Lockheed Martin Corporation (LMC) to investigate for various scenarios, the distribution of aerosol and particulate mass in a stabilized buoyant plume created as a result of a fireball explosion. The information obtained from these calculations is to provide background information for the radiological consequence analysis of the FSAR. Specifically, the information is used to investigate the mass distribution within the "cap and stem" portions of the initial fireball plume, a modeling feature included in the SATRAP module in the LMC SPARRC code. The investigation includes variation of the plume energy and the application of several meteorological conditions for a total of seven sensitivity case studies. For each of the case studies, the calculations were performed for two configurations of particle mass in the plume (total mass and plutonium mass).

Atmospheric dispersion of the plume was predicted by using the PUFF and MCK modules of the ERAD code [Boughton, 1992]. The ERAD code was developed at SNL to simulate the atmospheric dispersal of radioactive material when involved in a high explosive detonation. The PUFF code module is an integral plume rise code for high explosive detonations. The MCK module calculates particle dispersion as a stochastic process by applying a discrete time Lagrangian Monte Carlo method. In addition to the ERAD code modules, this study also implemented the SNL Fireball code [Dobranich, 1996], to simulate the fireball and aerosol physics of a postulated launch explosion that involves radioisotope thermoelectric generators (RTGs), which contain PuO_2.

The calculations for this study were performed for two plume particle mass configurations:

1) total plume mass – which includes particles of PuO_2, soot, entrained dirt and aluminum oxide (if aluminum structures involved in the accident are predicted to vaporize); and
2) PuO_2 mass only – which includes only particles of PuO_2.

In addition to the two particle mass configurations, the calculations were performed for seven sensitivity cases in which meteorology and the energy available for thermal rise were varied.

The results of this study suggest two basic models of the mass distribution in the cap and stem in a lofted plume. The first is the classical model of a cap and stem, for which the percentage of the plume mass contained in the cap and stem is about 80% and 20%, respectively. The second is a uniform distribution of the mass throughout the plume. Because of particle density differences, the mass distribution models indicated for the total plume mass configuration are different from the PuO_2 particle mass configuration (for this study, less than 0.1% of the plume mass is PuO_2).

In this study, the classical model of a cap and stem is indicated for four sensitivity cases for the total plume mass configuration, and for two sensitivity cases for the PuO_2 mass configuration. Fairly uniform distributions are indicated in the remaining sensitivity cases for both the total and PuO_2 mass configurations. For most of the cases for uniform PuO_2 mass distributions, a substantial amount of the PuO_2 mass in the plume is deposited on the ground (roughly 10%). The cap and stem model that is appropriate for each case not only depends on the particle density (heavy PuO_2 particles vs. lighter particles in the total plume) but also appears to depend on the H/D ratio. The H/D ratio is a measure of

the mixing layer penetration by the plume, where H is the simulated cloud height, and D is the mixing layer depth. In light of the results of this study, some suggested distributions were formulated to characterize the uncertainty associated with the fraction of PuO_2 mass in the plume that is contained in the stem. The suggested distributions are provided in Table 1.1 in terms of two specifications:

1. without a dependence on the H/D ratio, and
2. for three ranges of H/D ratios (H/D < 3, between 3-10, or > 10).

Also listed in Table 1.1 is the uncertainty distribution that was adopted in the Cassini FSAR.

Table 1.1 Distributions for the Fraction of PuO_2 Mass Contained in the Stem

Percentiles	Fraction of PuO_2 Mass in Stem				
	Cassini FSAR distribution	Suggested Updated Distributions			
		no H/D dependency	H/D < 3	3 < H/D < 10	H/D > 10
0th	0.03	0.05	0.2	0.05	0.15
5th	0.1	0.2	0.3	0.1	0.3
50th	0.2	0.6	0.7	0.2	0.4
95th	0.5	0.8	0.8	0.3	0.6
100th	0.6	0.9	0.9	0.5	0.75

In summary, this study indicates that consideration of the density of particles in a lofted plume is important in determining the distribution of mass within the plume. Compared to plumes with lighter particles, plumes with particles of higher density are predicted to accumulate more mass in lower elevations of the plume (significant amounts of the higher density particles may even be deposited on the ground). This study also indicates that the energy of the release relative to the mixing layer depth impacts the vertical mass distribution in a lofted plume. When the energy is sufficient to both penetrate the inversion layer and still loft the plume to elevations that are between about three and ten times the mixing layer depth, then the classical cap and stem approximation is deemed to be adequate. If the energy is more or less than sufficient, then it is better to assume a more uniform vertical distribution of the mass in the plume.

2.0 Method of Calculation

The approach used in this study was to calculate atmospheric dispersion of the plume by using two modules of the ERAD code [Boughton, 1992]. The ERAD code was developed at SNL to simulate the atmospheric dispersal of radioactive material when involved in a high explosive detonation. The ERAD code module, PUFF (Version 3.6S.3, 9/3/96) was modified by B. Boughton of SNL for stabilized plume studies in support of the Cassini Mission safety analyses. The PUFF code module is an integral plume rise code for high explosive detonations. Another ERAD code module, MCK (Version 3.6.1S.1, 9/3/96), was also applied in this study. MCK calculates particle dispersion as a stochastic process by applying a discrete time Lagrangian Monte Carlo method. In addition to the ERAD code modules, this study also implemented the SNL Fireball code (Version 1.2, 8/8/96) [Dobranich, 1997], which was developed at SNL specifically to support the Cassini Mission safety analyses. The SNL Fireball code simulates the fireball and aerosol physics of a postulated launch explosion that involves radioisotope thermoelectric generators (RTGs); the code simulation capability includes thermodynamics, chemistry, heat and mass transfer, vaporization, condensation and agglomeration.

The dataflow diagram for the software code modules that were implemented in this analysis is presented in Figure 2.1. The PUFF code module simulates the plume rise for a given set of atmospheric conditions and is executed once for each of the seven sensitivity cases. A sensitivity case numbered 'x' is designated in Figure 2.1 as 'case-x'. The SNL Fireball code is executed a single time for this study, providing the particle size transformation for the particles involved in a fireball explosion. Information can be obtained from the SNL Fireball code output that describes the final fireball particle size distribution in terms of either the total plume mass or the plutonium dioxide mass. Both the total mass and the plutonium dioxide mass configurations were utilized in this study and implemented as the two particle mass configurations.

The MCK code module requires the information generated by both the PUFF code module and the SNL Fireball code. The PUFF output can be utilized directly as input by MCK. The distribution of particle mass and size provided as SNL Fireball code output, however, is transformed into three distributions for each of the two particle mass configurations to be used as input by MCK. The three MCK input distributions for the '#' particle mass configurations are designated in Figure 2.1 as 'pmc#1,' 'pmc#2,' and 'pmc#3.' Thus, the input for a single execution of MCK consists of one set of three particle mass distributions from the SNL Fireball code and one sensitivity case output file from the PUFF module (the MCK input is discussed in more detail in Section 6.1). The information from the three MCK output files is then combined for each sensitivity case and each particle mass configuration to formulate the results of this analysis.

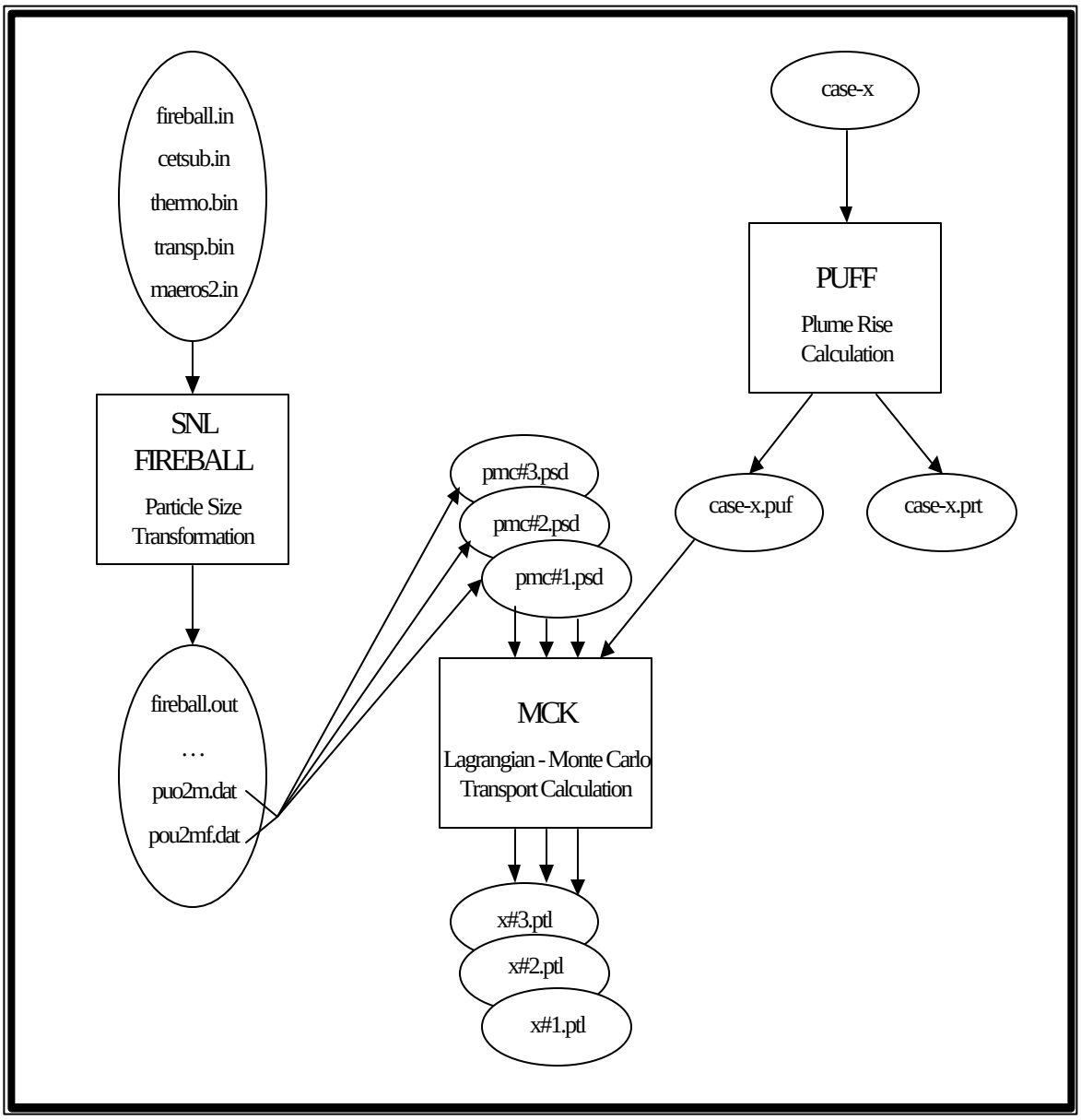

Figure 2.1 Cassini Sensitivity Analysis Dataflow Diagram.

3.0 Particle Mass Configuration and Sensitivity Case Definition

The calculations for this study were performed for two plume particle mass configurations:

1) total plume mass – which includes particles of PuO_2, soot, entrained dirt and aluminum oxide (if aluminum structures involved in the accident are predicted to vaporize); and
2) PuO_2 mass only – which includes only particles of PuO_2.

The total plume mass is utilized in this study to determine the overall applicability of a cap and stem model to a lofted plume. The inclusion of the second configuration of PuO_2 mass only serves two main purposes:

1) to study the effect of particle density upon mass distribution within the plume (PuO_2 particle density is about five times greater than the average density of all particles), and
2) to investigate the location of the plutonium oxide particles within the lofted plume (and thus, the location of the particles that result in radiation exposure).

Both particle mass configurations are obtained from a single execution of the SNL Fireball code (a separate SNL Fireball execution is not performed for only the PuO2 particles because inclusion of all particles in the fireball better represents actual accident conditions).

In addition to the two particle mass configurations, the calculations were performed for seven sensitivity cases in which meteorology and the energy available for thermal rise were varied. The seven cases were designed to be consistent with other analyses performed for the Cassini Mission FSAR, and were specified by N. Deane of LMC [Deane, 1996]. Table 3.1 provides a summary of the seven sensitivity cases by listing the sensitivity case number, a short qualitative description of the meteorology and the lofting energy available for thermal rise.

Table 3.1 Summary Description of the Sensitivity Cases.

Sensitivity Case Summary		
Case	Description of Meteorology	Lofting Energy Available (fireball type designator)
1	Maximum plume rise day	High (T2)
2	Minimum plume rise day	Moderate (T3)
3	Average plume rise day	High (T2)
4	Maximum mixing height day	Moderate (T3)
5	Minimum mixing height day	Moderate (T3)
6	Minimum wind shear day	Moderate (T3)
7	Maximum mixing height day	High (T2)

Two discrete lofting energy levels were applied in this study, the two levels relate to ground core fireball types T2 and T3, which are a core fireball and a space vehicle fireball, respectively, as defined in the Cassini Mission FSAR. The fireball type T2 involves higher release energy. Case 7 actually utilizes the same meteorology as Case 4, but implements the alternate lofting energy. More quantitative details regarding the sensitivity cases are provided in Section 5.1, which discusses the PUFF module input.

4.0 SNL Fireball Code Analysis

The SNL Fireball code determines the quantity and size distribution of plutonium-bearing particles released to the atmosphere that originate from the radioisotope thermoelectric generators (RTGs) consumed in a fireball explosion created during a launch accident. The SNL Fireball code provides an integrated simulation capability for modeling the many and varied processes involved in such an event, including: thermodynamics, chemistry, heat and mass transfer, vaporization, condensation, and agglomeration. The fireball physics model predicts temperature, composition, size, and rise velocity of the fireball by application of a single uniformly-mixed control volume. The fireball initiates as either a hemisphere at ground level or a sphere in air, and then rises while including buoyancy, drag, and volume effects, as well as combustion, air entrainment and heat loss. The SNL Fireball Code Version 1.2 (8/8/96) was implemented in this study.

4.1 SNL Fireball Code Input Parameters and Assumptions

A single execution of the SNL Fireball code was performed for this study, i.e., the output from one calculation applied to all the sensitivity cases. Inputs to the code were designed to be consistent with other analyses performed for the Cassini Mission FSAR, and were specified by C. Chang of LMC [Chang, 1996]. The Fireball calculation was performed for a ground level fireball with 10 grams of PuO_2 involved in the accident. Selected input parameters implemented in this study are listed in Table 4.1.

The Weibull distribution noted in Table 4.1 is used in the SNL Fireball code to provide the initial particle mass fractions for each particle bin. The Weibull distribution parameters are not code inputs but are assigned within the code itself. For this study, the Weibull distribution parameters α and β were set to the values as specified for the Cassini Mission FSAR LASEP-T Weibull parameters. The Weibull cumulative distribution function, $F(\omega)$ is expressed as:

$$F(\omega) = 1 - \exp(-(\omega/\beta)^{\alpha}), \qquad 0 \le \omega \le \infty$$

Where:

ω = aerosol diameter, cm

β = 0.322297 * escfrac * rupture
- escfrac = fraction of PuO_2 particles with diameter < rupture that escape = 1.0
- rupture = rupture diameter = 1 cm

α = 0.9976

Table 4.1 Fireball Calculation Input Parameters

Selected Parameter Inputs to the Fireball Code	
mass of PuO_2 injected into fireball (RTG mass)	10 g
rupture diameter	1 cm
fraction of PuO_2 particles w/ diameter < rupture that escape	1.0
ambient temperature	298 K
fireball combustion product pressure	1 atm
initial elevation of the center of the fireball	0.0 cm
initial mass of soot added to the fireball	100 g
diameter of generated soot particles	2.2e-5 cm
total aluminum alloy structural mass in fireball	1.58e7 g
diameter of generated aluminum oxide particles	5.0e-6 cm
initial mass of dirt injected to the fireball	0.0 g
diameter of entrained dirt particles	5.0e-5 cm
dynamic shape factor of all particles	1.2
volumetric PuO_2 heat generation rate	2.65 W/cm^3
PuO_2 melt temperature	2698 K
number of aerosol particle bins	14
number of rock particle bins	7
min aerosol particle diameter	1.0e-6 cm
max aerosol (or min rock) particle diameter	1.0e-2 cm
max rock particle diameter	1.0 cm
Weibull distribution parameters	LASEP-T

The CETSUB module of the SNL Fireball code simulates the combustion chemistry and thermodynamics of the launch accident. The CETSUB module is a modified version of the CET89 computer code developed by NASA [McBride, 1989]. The reactant mix input parameters to the CETSUB module are listed in Table 4.2 (C. Chang of LMC also specified the reactant mix inputs). The burn duration time input to CETSUB is 5.04 seconds.

Table 4.2 Fireball Reactant Mix

Reactant Mix for Fireball Calculation, Burn Duration = 5.04 s				
Reactant Name	Chemical Formula	Inventory (mol)	Enthalpy (J/mol)	Fuel/Oxidant
Nitrous Oxide	N_2O_4	1.34E+06	-1.96E+04	O
Unsymmetrical Dimethyl Hydrazine (UDMH)	$C_2H_8N_2$	1.10E+06	4.98E+04	F
Liquid Oxygen	O_2	5.43E+05	-1.30E+04	O
Liquid Hydrogen	H_2	1.72E+06	-9.00E+03	F
Monomethyl Hydrazine (MMH)	CH_6N_2	2.45E+04	5.40E+04	F
Hydrazine	N_2H_4	4.15E+03	5.06E+04	F

4.2 Fireball Calculation Results

The SNL Fireball code assigns a particle to a bin based on its diameter. Initially, all particles in each bin are assigned the geometric mean diameter of the bin, but the particle bin diameters change as vaporization (particle size decreases) and condensation (particle size increases) occur. If the minimum or maximum particle size boundaries of a bin are crossed, then the mass in the bin is moved to a higher or lower particle bin. The SNL Fireball code aerosol bin assignment is based on the defined aerosol and rock boundaries listed in Table 4.1, a geometric constraint on bin boundaries, and the number of bins. Table 4.3 lists the minimum, maximum, and geometric mean diameter of the aerosols in each bin, as determined by the SNL Fireball code.

The fireball calculation terminates at a simulated time of 33 seconds. The initial fireball radius is calculated as 1.36 m, the fireball radius at 33 seconds is calculated as 194 m. The final elevation of the center of the fireball is 944 m. The calculation predicts the generation of about 10,800g of soot within the fireball and the entrainment of about 1500g of dirt over the simulation time.

The temperature of the aluminum structures remains below the alloy melting temperature and thus there is no aluminum alloy vaporized during the simulation. The SNL Fireball code assumes 7075-T6 aluminum alloy with a melting temperature of 933.2 K. Out of the five aluminum alloy structures, only a single structure is predicted to attain temperatures that approach the melting temperature at the

termination of the simulation.

Table 4.3 Fireball Aerosol Bins for this Study

Fireball Aerosol Bin Classification			
Bin	Min Dia (cm)	Max Dia (cm)	Geom Mean Dia (cm)
1	1.00E-06	1.93E-06	1.39E-06
2	1.93E-06	3.73E-06	2.68E-06
3	3.73E-06	7.20E-06	5.18E-06
4	7.20E-06	1.39E-05	1.00E-05
5	1.39E-05	2.68E-05	1.93E-05
6	2.88E-05	5.18E-05	3.73E-05
7	5.18E-05	1.00E-04	7.20E-05
8	1.00E-04	1.93E-04	1.39E-04
9	1.93E-04	3.73E-04	2.68E-04
10	3.73E-04	7.20E-04	5.18E-04
11	7.20E-04	1.39E-03	1.00E-03
12	1.39E-03	2.68E-03	1.93E-03
13	2.68E-03	5.18E-03	3.73E-03
14	5.18E-03	1.00E-02	7.20E-03

The initial and final distribution of total mass in the fireball is shown for the 14 particle bins in Figure 4.1 on a linear scale and in Figure 4.2 on a logarithmic scale. The initial and final distribution of PuO_2 mass in the fireball is shown for the 14 particle bins in Figure 4.3 on a linear scale and in Figure 4.4 on a logarithmic scale.

Initially, the total mass in the fireball consists of the soot in bins 5 and 6 plus the PuO_2 mass which is distributed across all the particle bins by applying the specified Weibull distribution as discussed in Section 4.1. The PuO_2 mass is vaporized out of bins 1 through 6 during the first timestep of $1x10^{-5}$ seconds, when the fireball temperature is at its peak of ~2850 K. At about 6 seconds into the simulation, all the particle bins experience an increase in PuO_2 by heterogeneous condensation, with the bulk of the PuO_2 particle mass at this point favoring bins 14, 13, 5 and 1 (in that order). The addition of more soot particles, the entrainment of dirt particles, and agglomeration of smaller PuO_2 particles with soot and dirt then adds many particles into bins 5 and 6. At the end of the simulation (33 seconds), the bulk of the total mass (mostly soot and dirt) is concentrated in bins 5 and 6 (~100%). (Recall that at the end of the simulation, more than 12,000g of the mass in the fireball is attributable to soot and dirt, whereas only 10g of mass is attributable to PuO_2.) At the end of the simulation, the bulk of the PuO_2mass (61%) is concentrated in bins 13 and 14. Most of the remainder of the PuO_2 mass (32%)

resides in bin 5 where heterogeneous condensation and agglomeration with other particles has occurred. Figure 4.5 provides the initial and final average density of the particles in the bins. Figure 4.5 illustrates that the bins that contain mostly non-PuO_2 particles are bins 5 and 6 initially, and bins 5 through 8 at simulation end. Essentially all the particles in the remaining bins are PuO_2 particles (density of 9.8 g/cm^3).

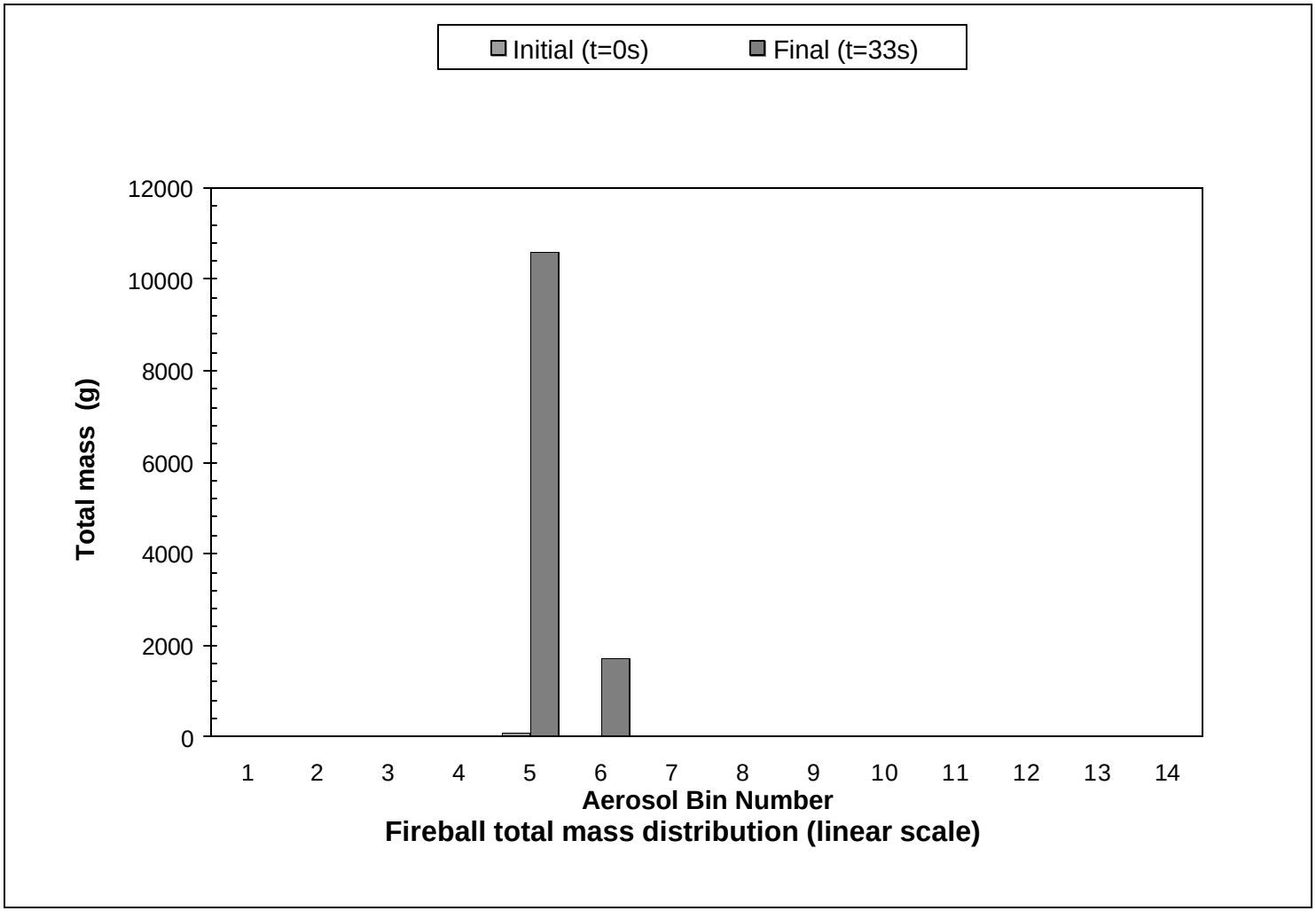

Figure 4.1 Initial/Final Distribution of Total Fireball Mass (linear scale)

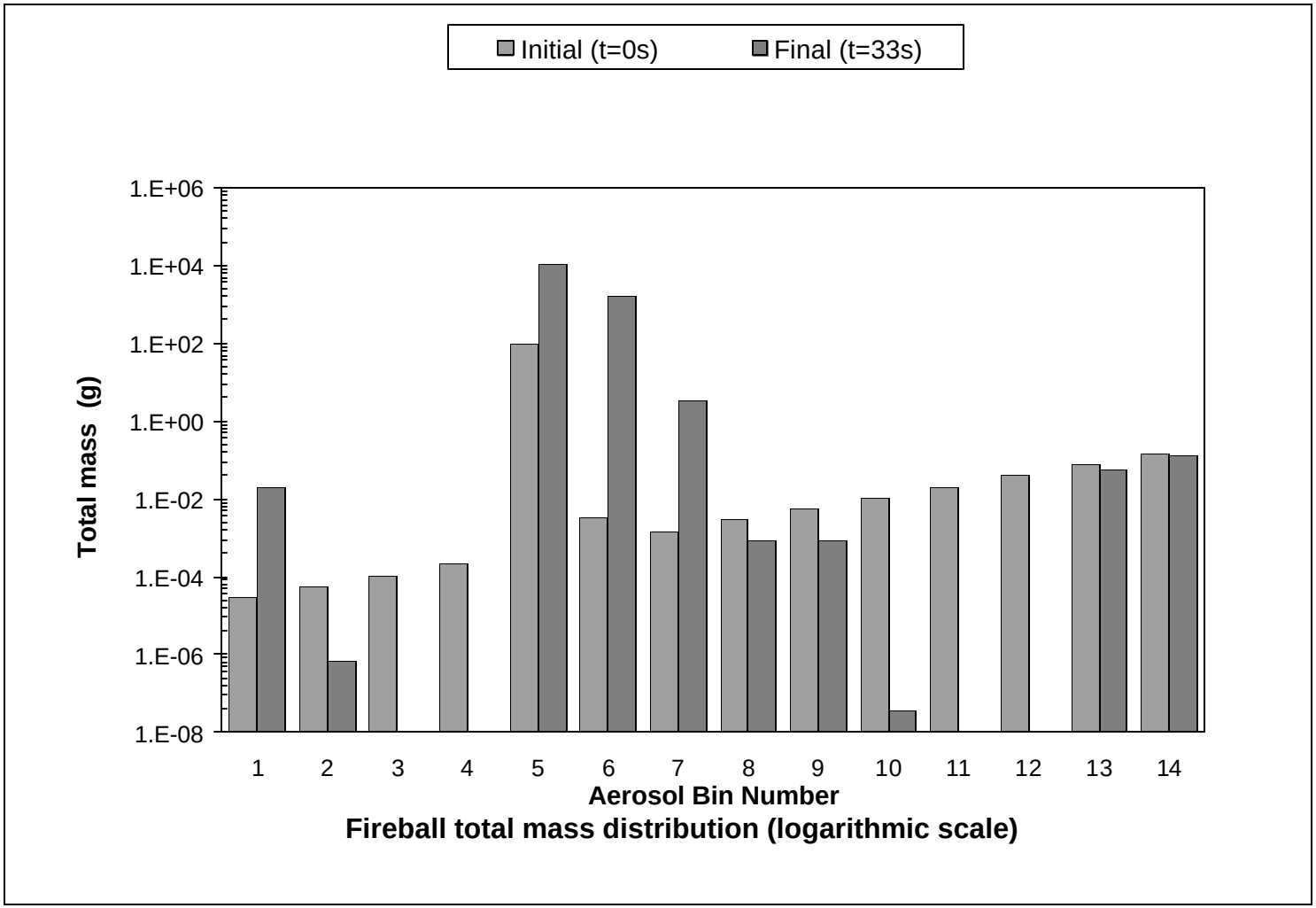

Figure 4.2 Initial/Final Distribution of Total Fireball Mass (logarithmic scale)

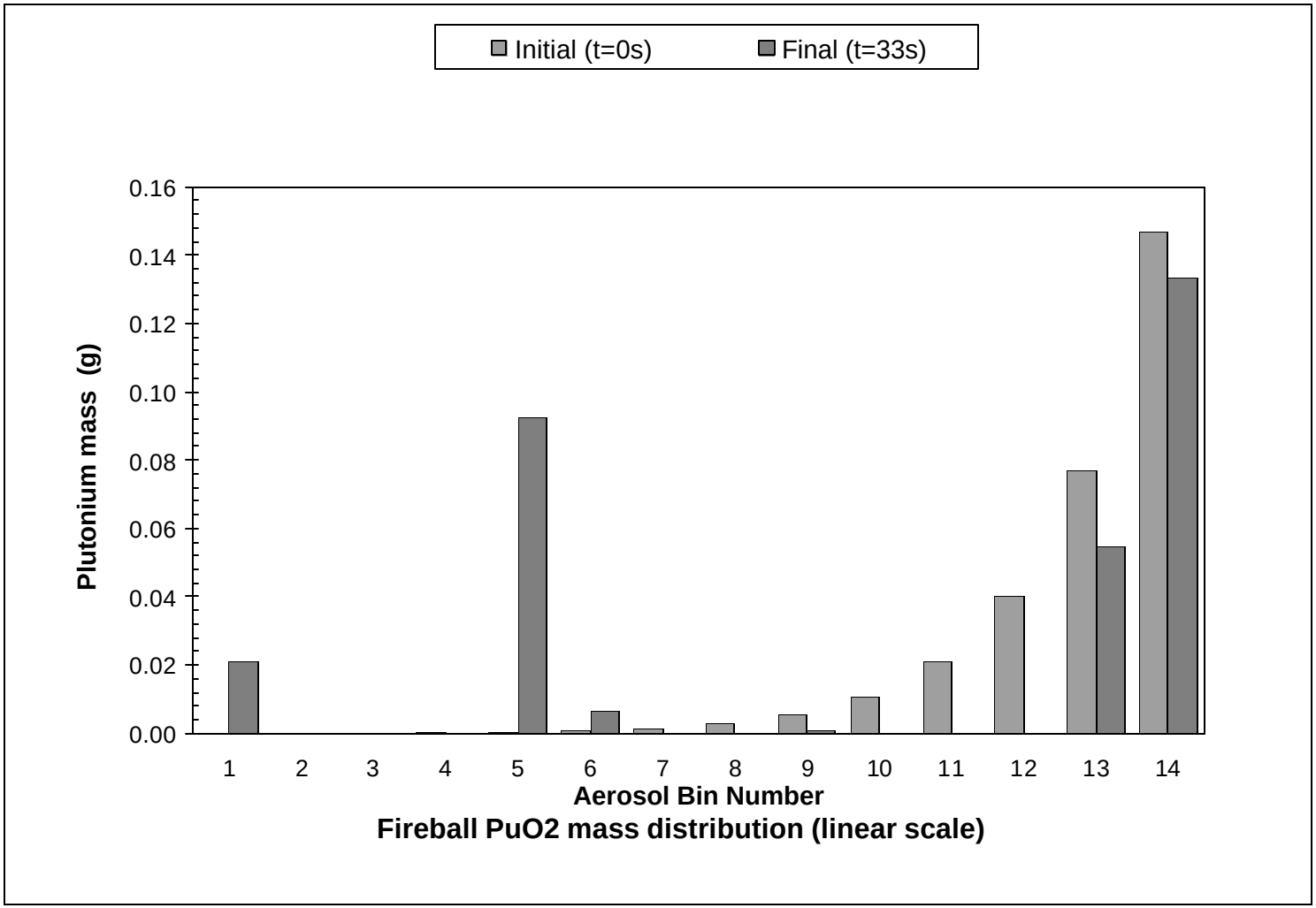

Figure 4.3 Initial/Final Distribution of PuO_2 Fireball Mass (linear scale)

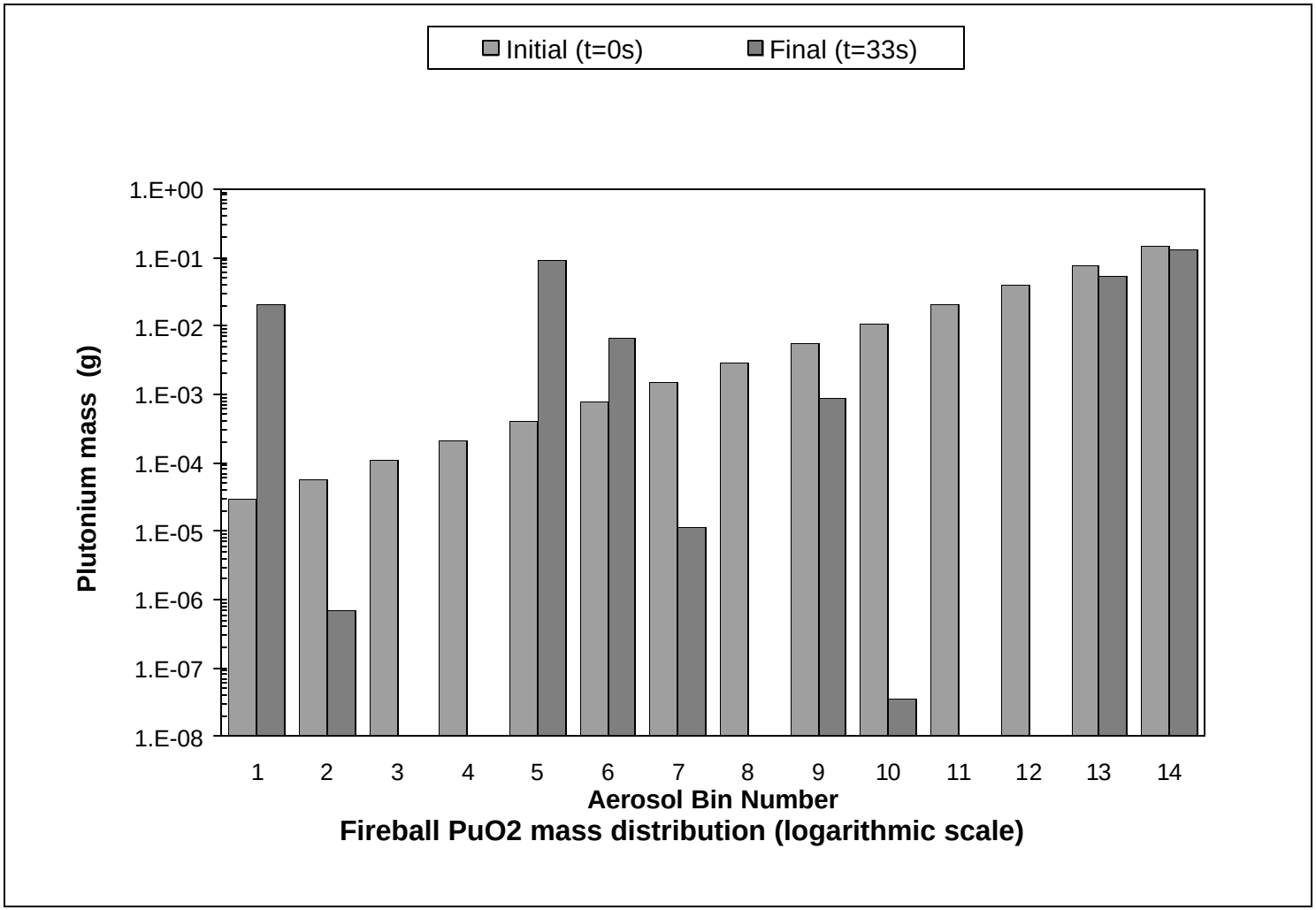

Figure 4.4 Initial/Final Distribution of PuO_2 Fireball Mass (logarithmic scale)

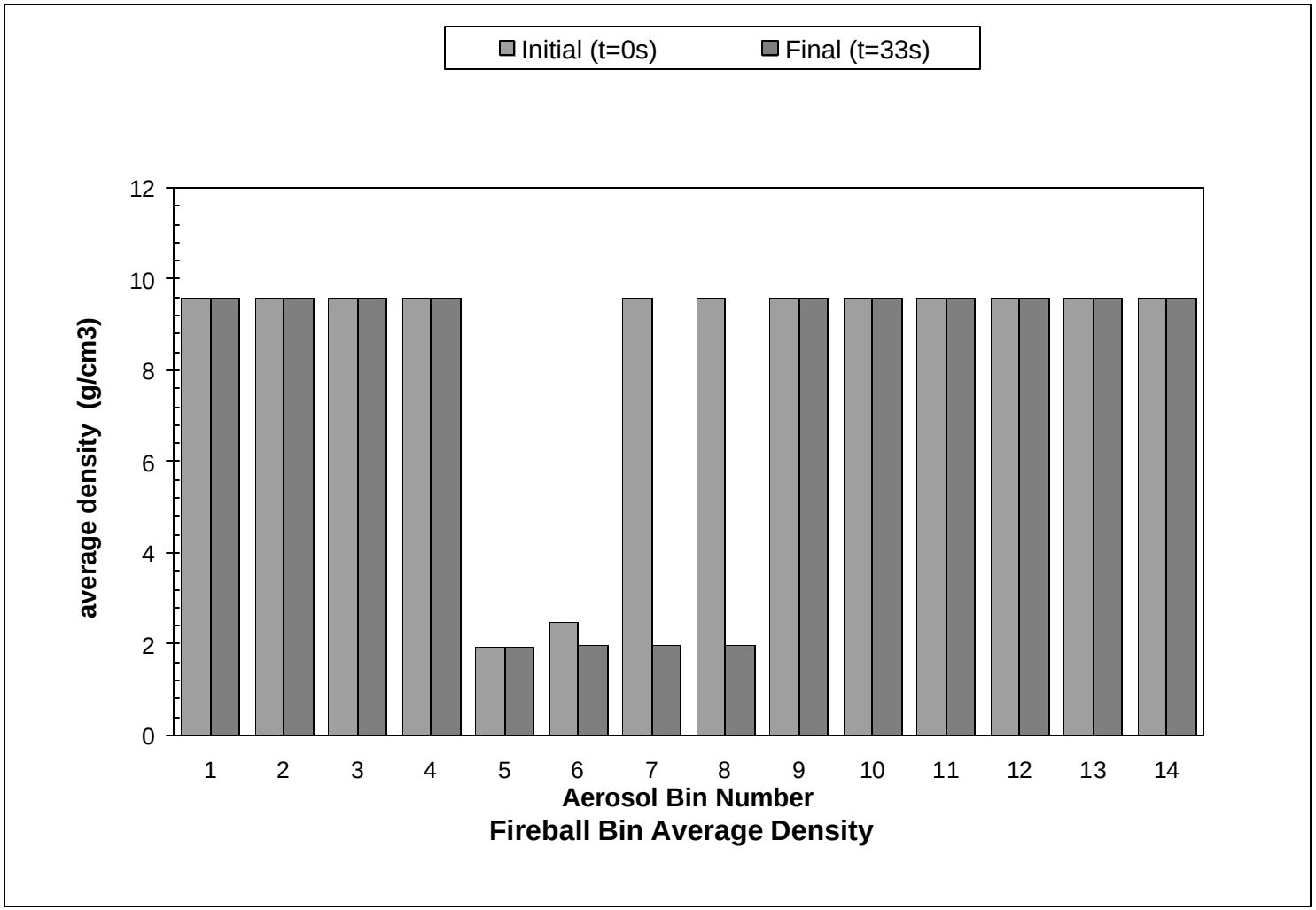

Figure 4.5 Initial/Final Average Density Distribution in Fireball

This page intentionally left blank.

5.0 PUFF Code Module Analysis

The PUFF code module is an integral plume rise code for high explosive detonations. The governing equations in PUFF are obtained by integrating the three-dimensional partial differential conservation equations for mass momentum and energy across the cloud cross-section. The integral equations are simplified to a set of coupled ordinary differential equations based on the cloud centerline variables, by neglecting some of the internal details of the plume and modeling only the macroscopic characteristics of the plume. The simulated cloud is composed of an equilibrium mixture of dry air, water vapor and liquid water; particulate material and gases are neglected since they constitute a very small fraction of the thermal mass. The physical and thermodynamic properties of the gaseous cloud are modeled as functions of time, while accounting for density stratification in the ambient atmosphere and wind cross flow.

5.1 PUFF Input Parameters and Assumptions

The input required for PUFF includes the energy in the plume available for thermal rise as well as the meteorological conditions such as: roughness length, ground-level pressure, relative humidity, height of lowest inversion, precipitation rate, and ambient temperature and wind speed profiles. N. Deane of LMC provided the input data specifications for the PUFF module to SNL. Table 5.1 summarizes some quantitative information included in the PUFF input for the seven sensitivity cases. For all sensitivity cases, the surface roughness length is specified as 5 cm, the precipitation rate is 0.0 mm/hr, and the release elevation is at 0.0 m above ground level. The lofting energies include two discrete energy levels, 5.0×10^{11} J and 7.1×10^{9} J, which relate to the LMC fireball types T2 and T3, respectively. The meteorological conditions specified for each sensitivity case are actual data from the Kennedy Space Center (KSC) site for specific dates and times. The data for all cases are obtained from days in October (cases 1, 3-7) and November (case 2), at times of 3 a.m. (cases 4, 6, 7) and 7 a.m. (cases 1, 2, 3, 5). Case 7 actually utilizes the same meteorology as Case 4, but implements the alternate lofting energy. The ambient temperature and wind profile data in the input files extend to an elevation of 28000 m above ground level, although for this application, elevations below about 7000 m are of interest.

5.2 PUFF Results

The PUFF module simulates the plume rise until the time that the cloud becomes stabilized (vertical velocity component is less than 0). Information that can be obtained from the PUFF module output includes a time history of cloud physical size and location, such as height, radius, horizontal position (E/W and N/S location), and vertical velocity. The PUFF module provides thermodynamic properties of the cloud such as density, temperature, mass fraction dry air, and quality. Additional meteorological summary information can also be obtained in terms of the mixing depth calculated in PUFF, and information to obtain the Pasquill stability class.

Table 5.1 Selected PUFF Input Data

PUFF Module Input Information								
Case	Description of Meteorology	Lofting Energy Avail (J)	Wind speed at elev above ground			Surface Temp. (C)	Relative Humidity	Inversion Height (m)
			0 m elev	200 m elev	1000 m elev			
1	Max plume rise day	5.0E+11	2.2	4.72	8	19.4	0.992	145
2	Min plume rise day	7.1E+09	1.5	6.59	5.26	12.6	0.734	135
3	Avg plume rise day	5.0E+11	7.2	7.98	6.73	21.1	0.585	485
4	Max mixing height day	7.1E+09	11.2	20.9	16.2	22.2	0.903	884
5	Min mixing height day	7.1E+09	0.9	5.85	6.72	23.7	0.931	77
6	Min wind shear day	7.1E+09	5.3	7.66	8.09	26.3	0.828	406
7	Max mixing height day	5.0E+11	11.2	20.9	16.2	22.2	0.903	884
All cases: surface roughness lenth = 5 cm, precipitation rate = 0.0 mm/hr, release at 0.0 m elevation								

Table 5.2 provides some summary information obtained from the PUFF module output for each sensitivity case. The Pasquill stability class is shown for two methods of determination, the inverse Monin-Obukhov length (Inv M-O) and the vertical temperature gradient (dT/dz). The PUFF code module applies Monin-Obukhov surface layer similarity theory, and thus implements the inverse Monin-Obukhov length in its calculations (the vertical temperature gradient is provided here as additional information to the reader). The stability classes for cases 1, 3, 4, 6 and 7 are indicated as neutral to slightly stable; whereas, for cases 2 and 5, the stability classes are indicated as moderately stable to stable. For convective and neutral conditions, PUFF models the mixing layer depth as the height of the lowest inversion, however, in a stable boundary layer, buoyancy forces suppress turbulence, reducing the mixing depth to a height less than that of the ground-based inversion. This is demonstrated in Table 5.2, where for all cases except 2 and 5, the depth of the mixed layer is equal to the lowest inversion height indicated in Table 5.1, and for cases 2 and 5, the mixed layer depth is less than the lowest inversion height.

Table 5.2 Selected PUFF Output Data

Selected PUFF Output											
Case	Description of Meteorology	Lofting Energy Avail (J)	Pasquill Stability Class		Depth of Mixed Layer (m)	PUFF simulation time (sec)	PUFF init plume dia, d_i (m)	PUFF final plume dia, d_f (m)	PUFF plume rise, H_r (m)	Cloud center, H_c[1] (m)	Stem column height, H_s[2](m)
			Inv M-O	dT / dz							
1	Max plume rise day	5.0E+11	E	E	145	2040	250	3390	6600	5810	4120
2	Min plume rise day	7.1E+09	F	G	34	110	60	170	310	270	190
3	Avg plume rise day	5.0E+11	D	E	485	240	250	900	1520	1340	890
4	Max mixing height day	7.1E+09	D	E	884	330	60	340	640	560	390
5	Min mixing height day	7.1E+09	F	F	34	480	60	340	780	690	520
6	Min wind shear day	7.1E+09	D	E	406	420	60	370	850	750	570
7	Max mixing height day	5.0E+11	D	E	884	330	250	1030	1780	1570	1060

[1] $H_c = .88 \times H_r$

[2] $H_s = H_c - d_f/2$

Table 5.2 contains the simulated plume rise time, and the PUFF plume diameter at both the initial and final plume simulation time. The PUFF plume rise, H_r, reported in Table 5.2 is the maximum simulated height of the cloud centerline; i.e., not including the cloud top. A factor of 0.88 is applied to the H_r calculated in the PUFF code module to calculate the vertical elevation the cloud center, H_c, in the Cassini FSAR SPARRC fireball plume model. The value of H_c is also reported in Table 5.2. An additional parameter, H_s, is reported in Table 5.2. H_s is the plume stem column height as implemented in the SPARRC model (more detail about the SPARRC plume model is provided in the Cassini FSAR, Vol. III, Section 3.5). H_s is provided in Table 5.2 to define the stem height in order to determine the amount of plume mass that is contained in the stem.

Note that for all cases except case 4, the plume rise attains elevations higher than the inversion cap and mixing layer (the case 4 plume rise is 640 m and the mixed layer depth is 884 m). The simulation for case 7, which is the case 4 meteorology with the higher buoyant energy release, shows that a more energetic release can loft the plume above the mixing layer for meteorological conditions that contain the plume under the mixing layer for a less energetic release.

This page intentionally left blank.

6.0 MCK Code Module Analysis

The MCK code module calculates particle dispersion as a stochastic process by applying a discrete time Lagrangian Monte Carlo method. The stochastic process approach provides a generalized model of particle dispersion as well as a fundamental treatment of buoyancy effects, droplet evaporation, calm winds, and time or space variability in meteorological conditions. The Monte Carlo simulation is implemented by following the trajectories of a few thousand individual particles. The probability density for particle trajectories satisfies a Fokker-Planck equation derived from the mass conservation equation for a passive aerosol. The displacement of each individual particle is derived from a set of stochastic differential equations.

6.1 MCK Input Parameters and Assumptions

The MCK code module requires the PUFF code module output, as well as the particle size and mass distribution within the initial plume. A total of 5000 particles were used in each of the MCK simulations performed for this study. The MCK code provides two options for particle size input: either by specification of a lognormal distribution of sizes or by singular application of independent sizes (polydispersed option vs. monodispersed option). The latter option requires the manipulation of many files (14 for each sensitivity case); and hence, if possible, it is more desirable to exercise the first option. On inspection of the particle distributions plotted in Figure 4.2, it is seen that not a single lognormal curve, but rather three, better represent the data. Thus, the total mass distribution is fitted with three lognormal distributions, and the MCK code module is executed three times for each sensitivity case. The MCK output is weighted by the fraction of total mass in each of the three particle bin groups to produce the total mass distribution throughout the plume. Table 6.1 lists the particle size distribution inputs to MCK for each bin group. The lognormal distribution is specified in terms of the 1^{st}, 50^{th}, and 99^{th} percentiles and the geometric standard deviation. Table 6.1 also lists the specific gravity for each bin group (based on the total mass within the group), and the weighting factor that is applied to each bin group in order to integrate the MCK results. To test the adequacy of the lognormal distribution fits for one of the sensitivity cases, the monodispersed option was exercised for the 14 bins and the results weighted by the fraction of the total mass in each bin. The results for vertical distribution of mass in the plume are almost identical for the two input options – the plotted curves are coincident and are therefore not included here.

In addition to studying the total mass distribution in the plume it is also of interest to investigate the atmospheric dispersion of the PuO_2 mass separately. The PuO_2 particle size distribution is approximated by simply adjusting the particle size distributions for the three lognormal distributions for the total cloud mass. The first and third particle size bin groups are not changed (because they consist of only PuO_2 particles), but the specific gravity for the second size category is changed, as well as the weighting fractions used in the integration of the results.

Table 6.1 MCK Particle Size Distribution Inputs for Total Mass Calculation

MCK Input for 3 Bin Specifications - Total Mass Calculation						
Bin Group	Particle size bins - lognormal curve fit parameters				Specific gravity	Bin Group Weighting Factor
	1%-ile (micrometers)	99%-ile (micrometers)	median dia (micrometers)	geometric std dev		
Bins 1-4	2.43E-03	1.12E-02	5.22E-03	3.28E-01	9.6	1.71E-06
Bins 5-12	3.98E-02	3.99E-01	1.26E-01	4.95E-01	1.95	0.999983
Bins 13-14	4.34E+01	6.92E+01	5.48E+01	1.00E-01	9.6	1.53E-05

Table 6.2 MCK Particle Size Distribution Inputs for PuO_2 Mass Calculation

MCK Input for 3 Bin Specifications - PuO_2 Mass Calculation						
Bin Group	Particle size bins - lognormal curve fit parameters				Specific gravity	Bin Group Weighting Factor
	1%-ile (micrometers)	99%-ile (micrometers)	median dia (micrometers)	geometric std dev		
Bins 1-4	2.43E-03	1.12E-02	5.22E-03	3.28E-01	9.6	6.80E-02
Bins 5-12	3.98E-02	3.99E-01	1.26E-01	4.95E-01	9.6	0.324
Bins 13-14	4.34E+01	6.92E+01	5.48E+01	1.00E-01	9.6	6.08E-01

6.2 MCK Results

For case 1, the MCK results for the vertical distribution of total mass and PuO_2 mass in the stabilized plume are plotted in Figures 6.1 and 6.2. These plots show the cumulative fraction of the mass versus elevation. Similar plots for the remaining cases are provided in Figures 6.2 through 6.14. For most cases, the vertical distribution of total mass is quite different from the distribution of PuO_2 mass (cases 2, 3 and 7 exhibit the most similarity between the total and PuO_2 mass distributions). For cases 1, 2, 3 and 5, the bulk of the total plume mass lies above the vertical center of the plume; while for cases 4, 6 and 7, the mass distribution is more uniformly distributed throughout the entire plume. The PuO_2 mass distributions show that a significant amount of the PuO_2 mass is at ground level (0 elevation) for cases 1, 4, 5 and 6, indicating less effective lofting of the higher density particles. Note that the maximum particle elevations plotted for the MCK calculation are not necessarily equal to the values reported for plume rise height, H_r in the PUFF output table, Table 5.2. Differences between the PUFF and MCK simulation occur as a result of the nature of the Monte Carlo simulation of individual particle behavior. However, the values from the two modules are within 5-10%, with the exception of case 4, which shows about a 20% disparity (recall that case 4 is the only case in which the mixing layer is not penetrated by the plume).

Table 6.3 lists some tabular information extracted from the MCK results for each sensitivity case and for both particle mass configurations. Included in Table 6.3 are the depth D of the mixed layer, the elevation H of the highest particle (MCK cloud height), and the ratio H/D. For both the total mass and the PuO_2 mass, Table 6.3 provides the fraction of plume mass contained in the plume stem and cap. The PuO_2 mass in the stem is presented both with and without the PuO_2 mass that is deposited on the ground. The fraction of mass in the plume stem for each case is determined by applying the stem column height, H_s, listed in Table 5.2, to the mass distributions as displayed in Figures 6.1 through 6.14. The amount of mass in the cap is then assumed to be the remainder of the mass located above the stem.

Table 6.3 Selected MCK Output

MCK Module Result Summary												
Case	Description	Energy (J)	Mixing layer depth, D (m)	MCK cloud height, H (m)	H / D	Fraction of total mass		Fraction of PuO_2 mass[1]		Fraction of PuO_2 mass[2]		
						in stem	in cap	in stem	in cap	On ground	in stem	in cap
1	Max plume rise day	5E+11	145	6140	42.3	0.26	0.74	0.66	0.34	0.12	0.54	0.34
2	Min plume rise day	7E+09	34	330	9.7	0.07	0.93	0.32	0.68	0.00	0.32	0.68
3	Avg plume rise day	5E+11	485	1560	3.2	0.20	0.80	0.31	0.69	0.00	0.31	0.69
4	Max mixing ht day	7E+09	884	830	0.9	0.70	0.30	0.86	0.14	0.23	0.63	0.14
5	Min mixing ht day	7E+09	34	760	22.4	0.16	0.84	0.67	0.33	0.10	0.57	0.33
6	Min wind shear day	7E+09	406	890	2.2	0.53	0.47	0.81	0.19	0.19	0.62	0.19
7	Max mixing ht day	5E+11	884	1830	2.1	0.61	0.39	0.76	0.24	0.02	0.74	0.24

[1] The stem mass includes the PuO_2 mass that is on the ground
[2] The PuO_2 mass on the ground is reported separately from the stem mass

In the variability-only analysis for the Cassini Mission FSAR, the fraction of plume mass that was assumed to be in the plume stem was 0.2; for the uncertainty analysis, the distribution of mass in the stem ranged from 0.03 to 0.60. Table 6.3 shows that for total plume mass, the FSAR uncertainty analysis is in good agreement with the uncertainty distribution (only case 4 is extremely outside of the distribution). For the PuO_2 mass in the plume, however, when the stem mass includes the PuO_2 ground deposit, only two of the sensitivity case results lie within the range of the distribution (cases 2 and 3). When the PuO_2 stem mass does not include the ground deposit, four of the sensitivity case results lie within the distribution range (cases 1, 2, 3 and 5), and only case 7 is extremely outside of the distribution. The results in the table indicate that there may be a relationship of the total mass fraction contained within a certain height to the H/D ratio. H/D ratios closer to unity represent conditions in which the buoyant forces in a plume are not strong enough to penetrate the mixing layer (or lowest inversion layer). On the other hand, the higher H/D ratios represent strongly driven buoyant plumes that penetrate the inversion layer and become trapped above it.

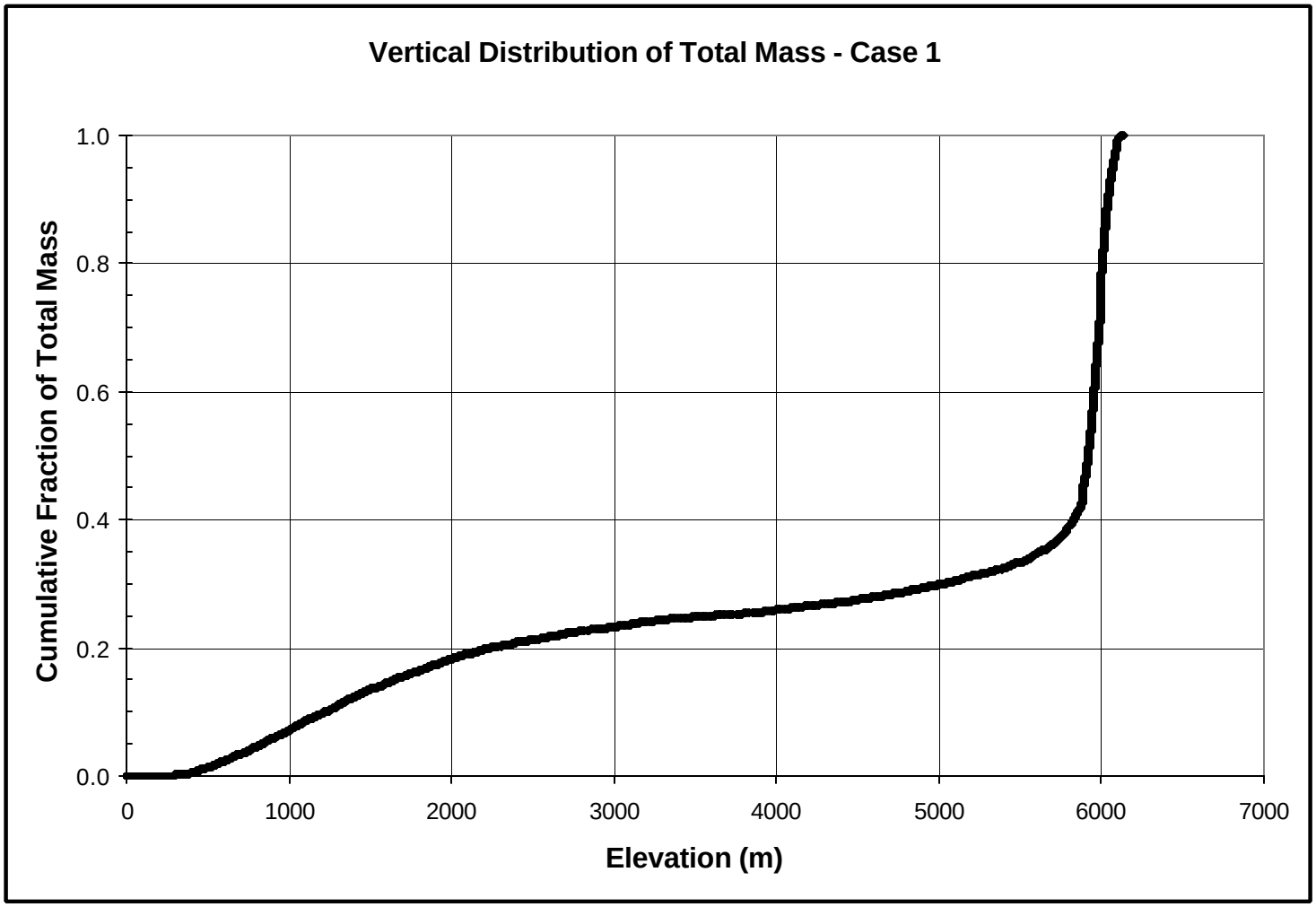

Figure 6.1 Case 1 - Vertical Distribution of Total Mass in Plume

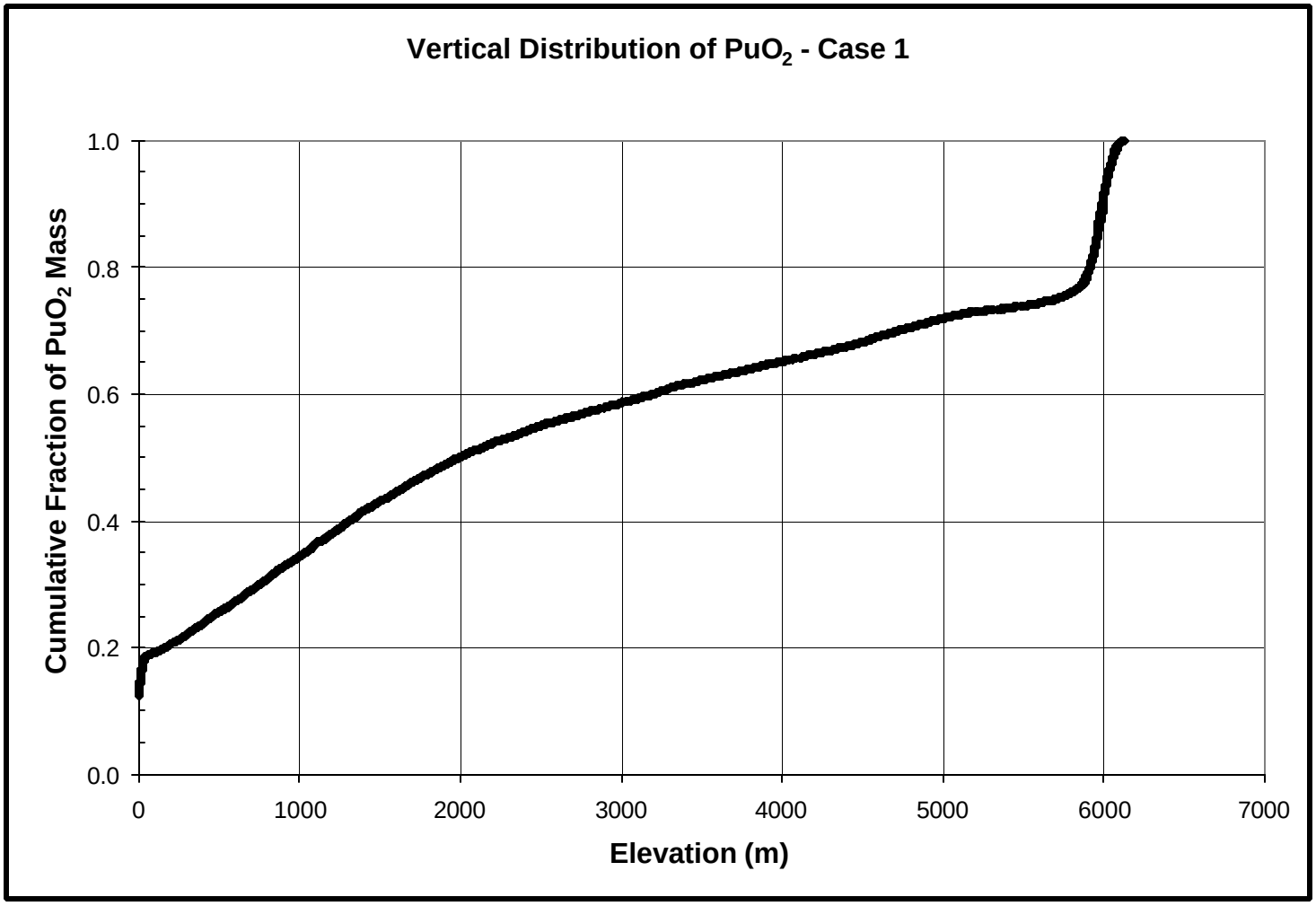

Figure 6.2 Case 1 - Vertical Distribution of PuO_2 Mass in Plume

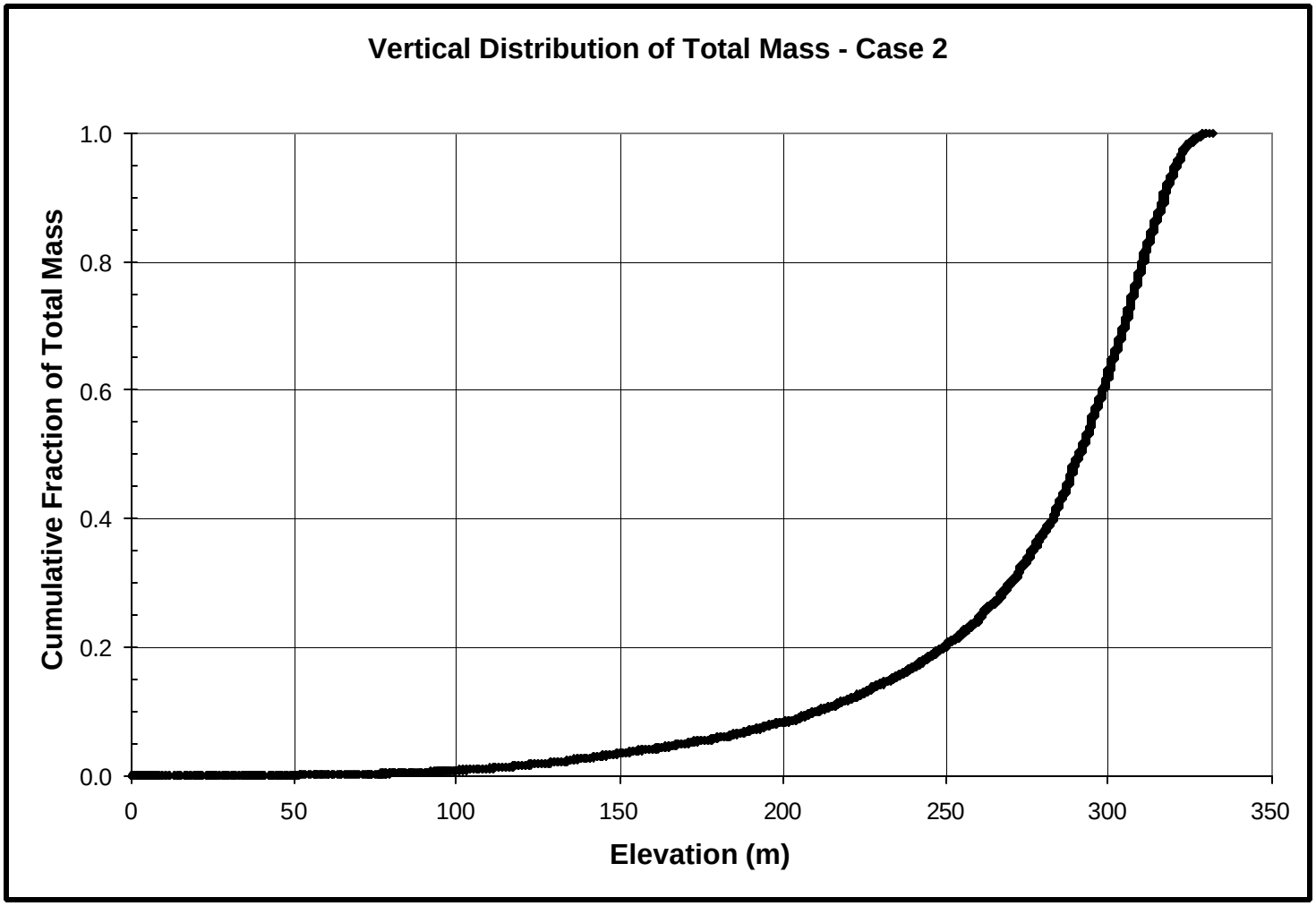

Figure 6.3 Case 2 - Vertical Distribution of Total Mass in Plume

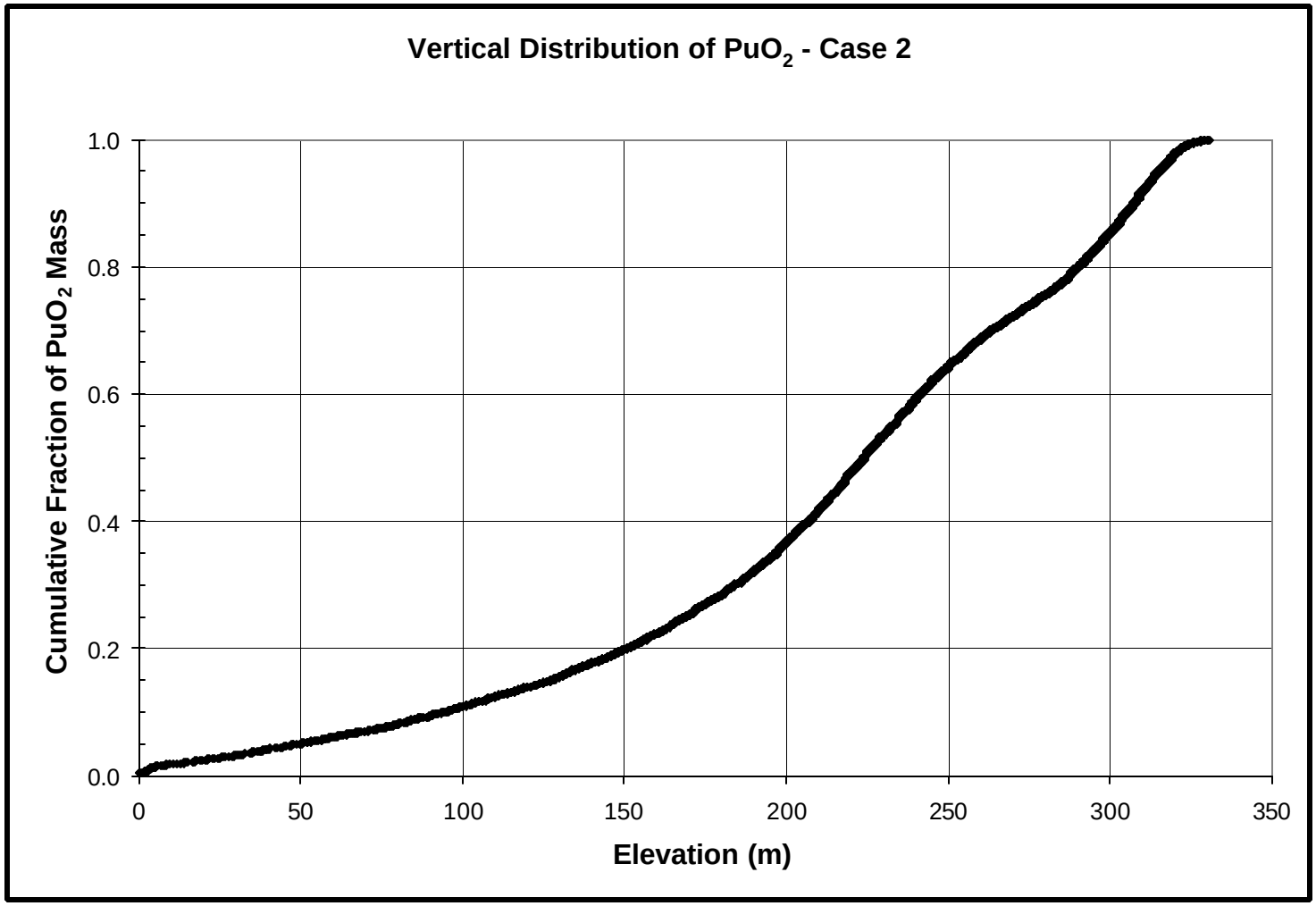

Figure 6.4 Case 2 - Vertical Distribution of PuO_2 Mass in Plume

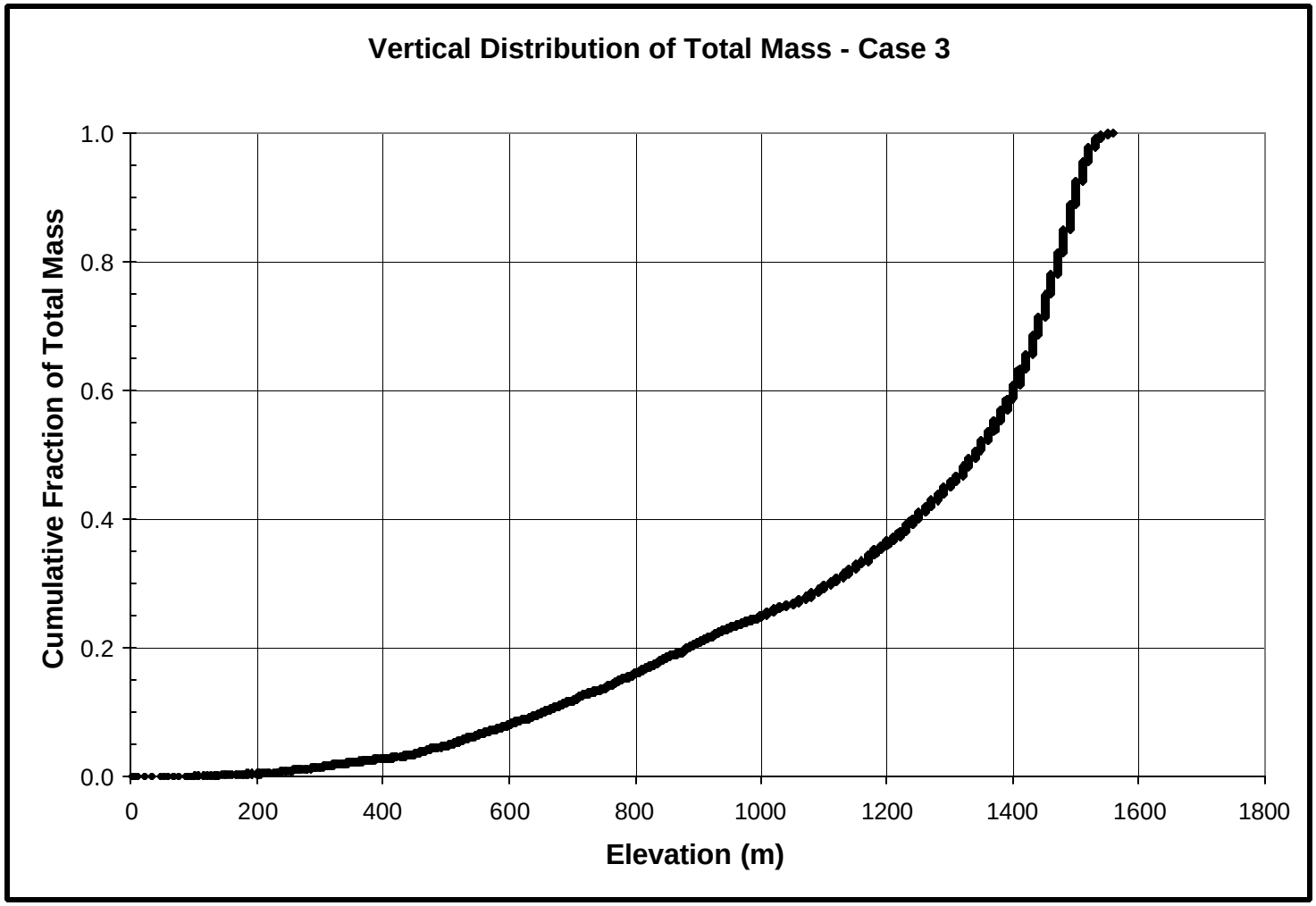

Figure 6.5 Case 3 - Vertical Distribution of Total Mass in Plume

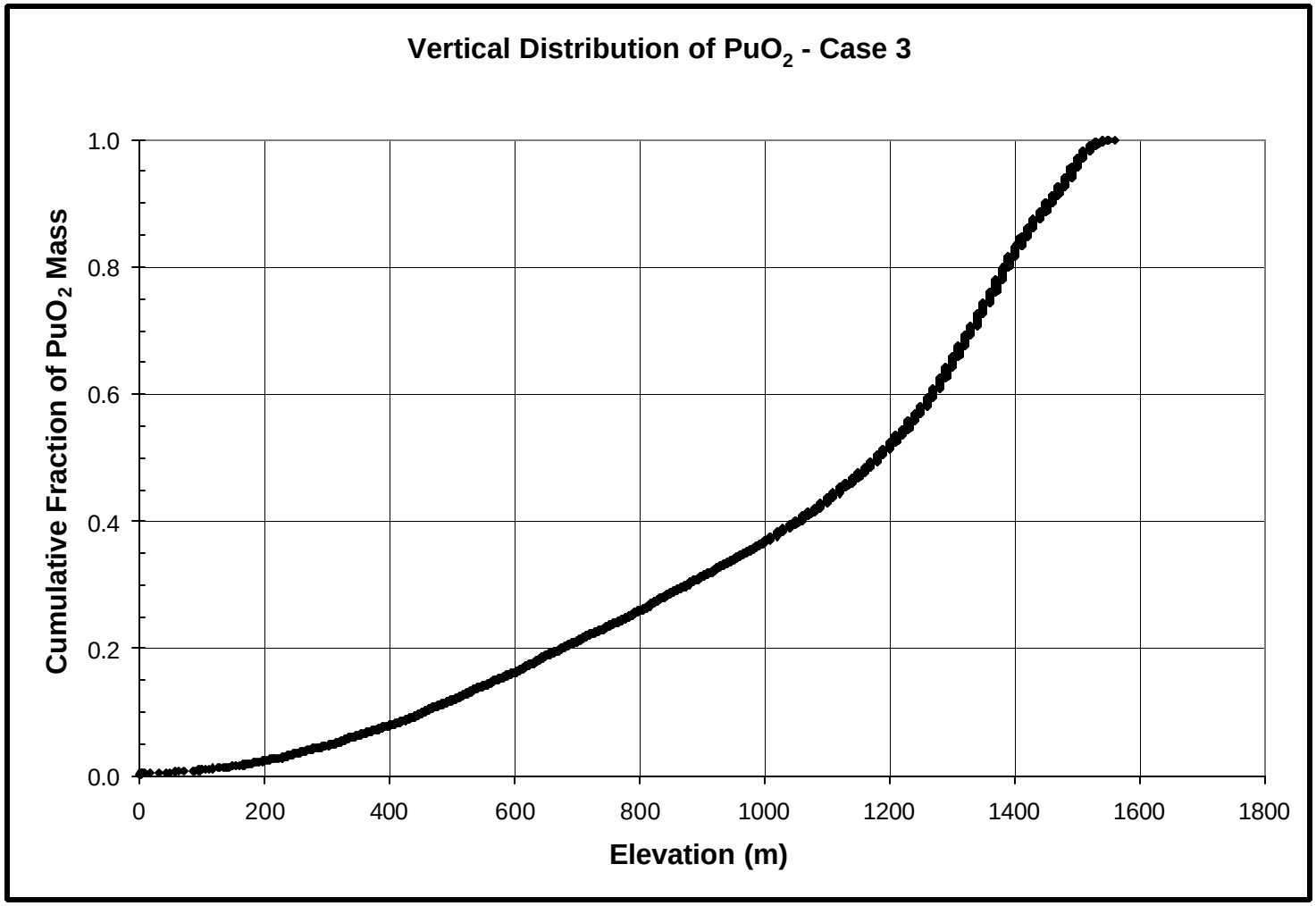

Figure 6.6 Case 3 - Vertical Distribution of PuO_2 Mass in Plume

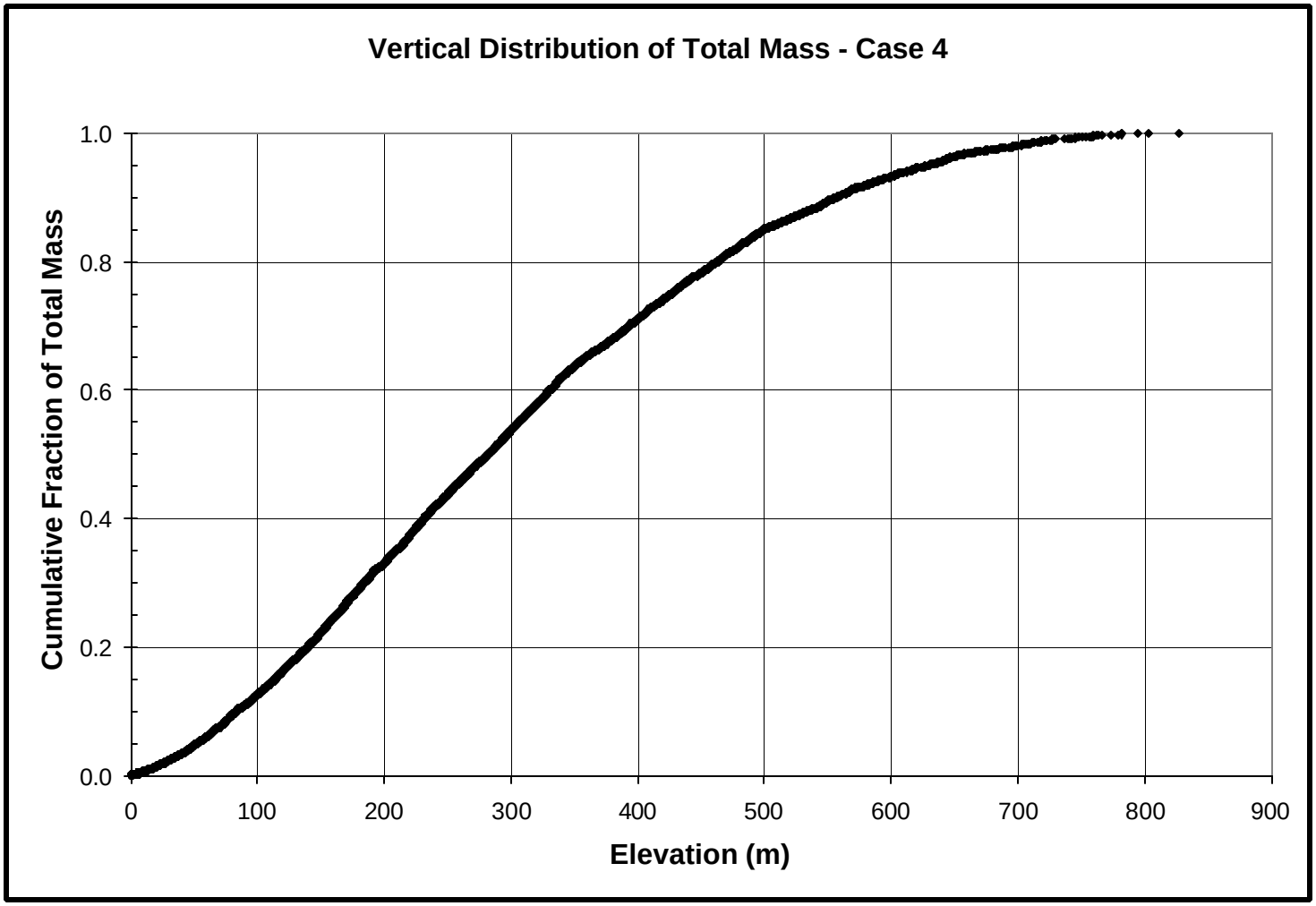

Figure 6.7 Case 4 - Vertical Distribution of Total Mass in Plume

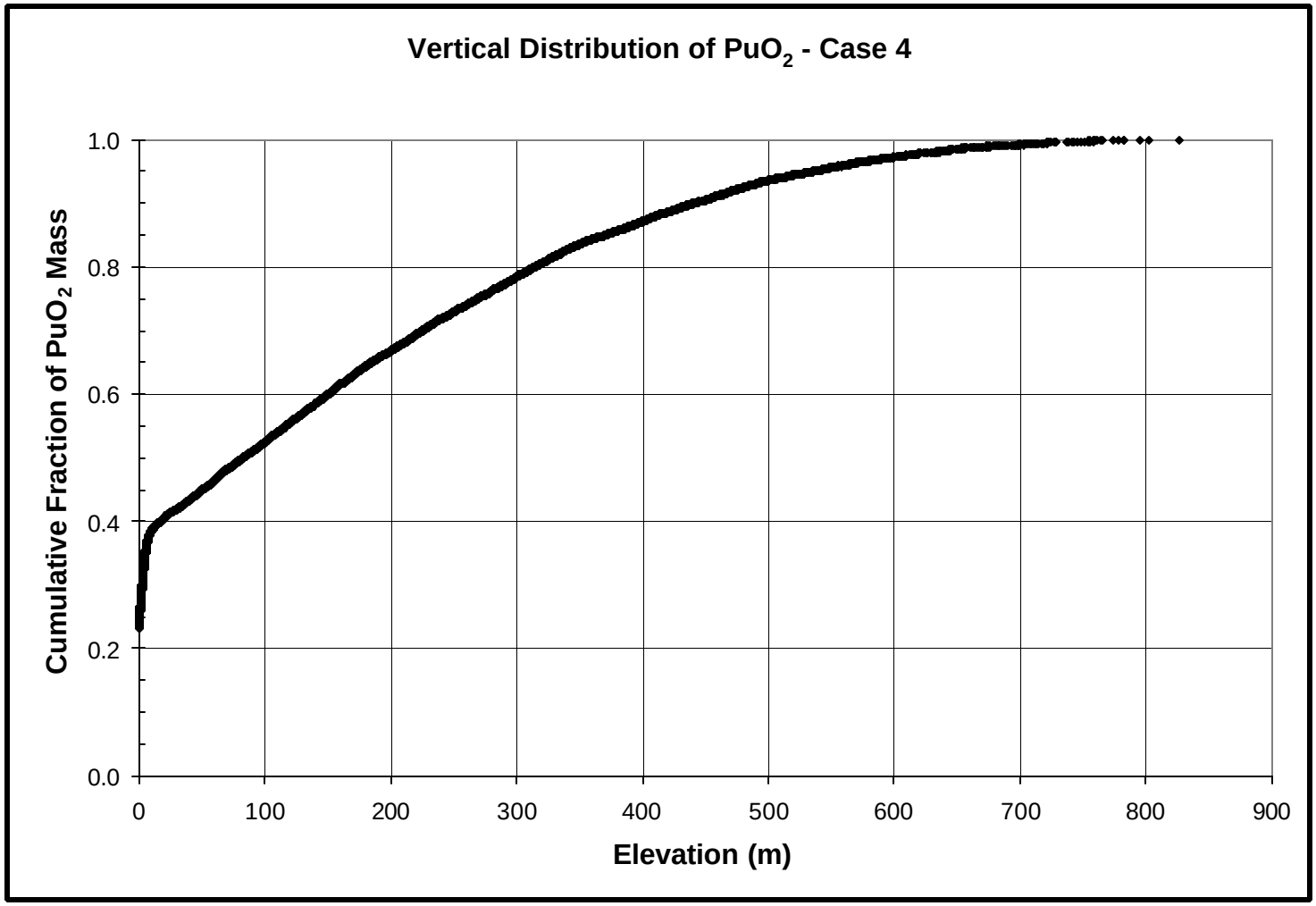

Figure 6.8 Case 4 - Vertical Distribution of PuO_2 Mass in Plume

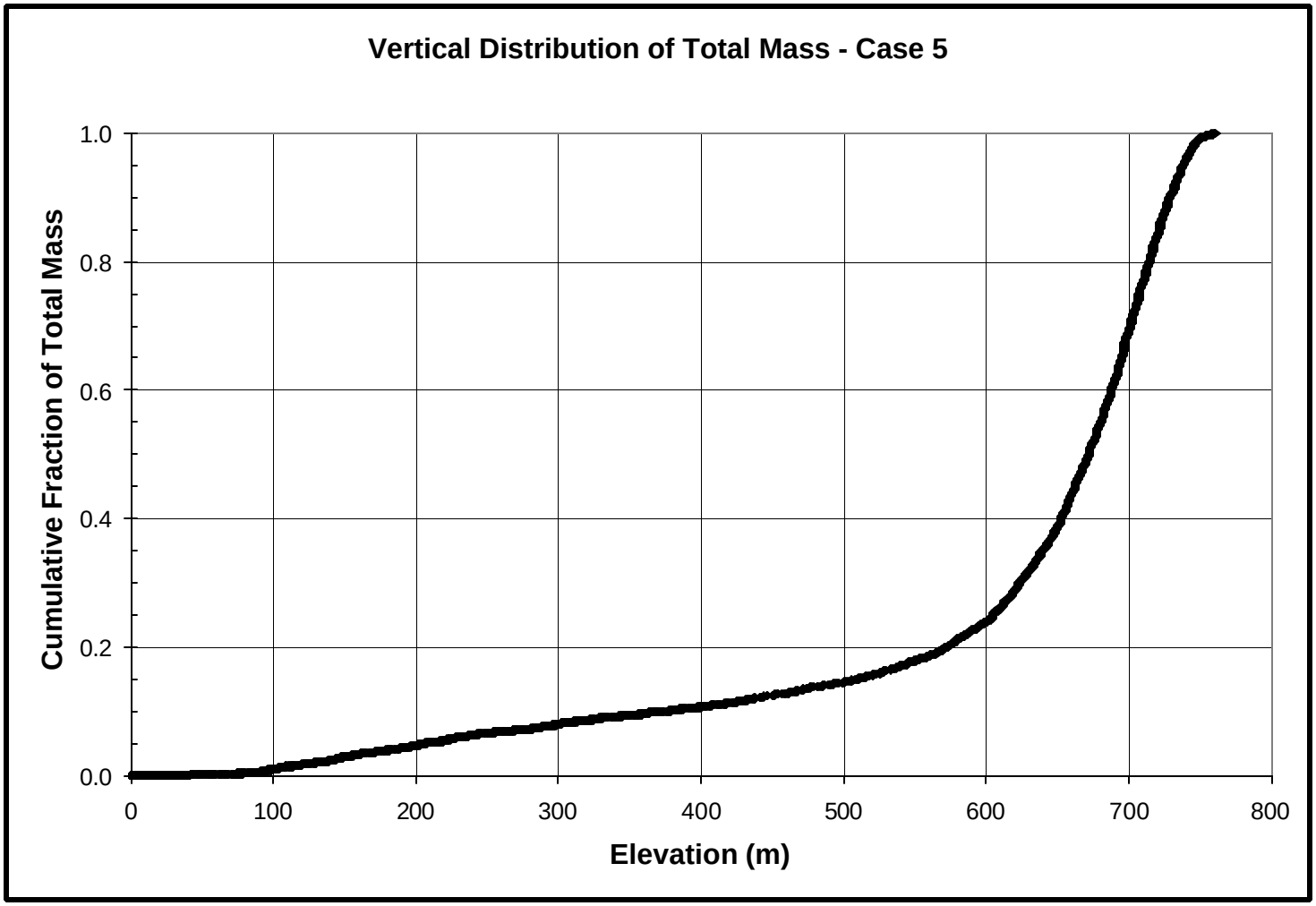

Figure 6.9 Case 5 - Vertical Distribution of Total Mass in Plume

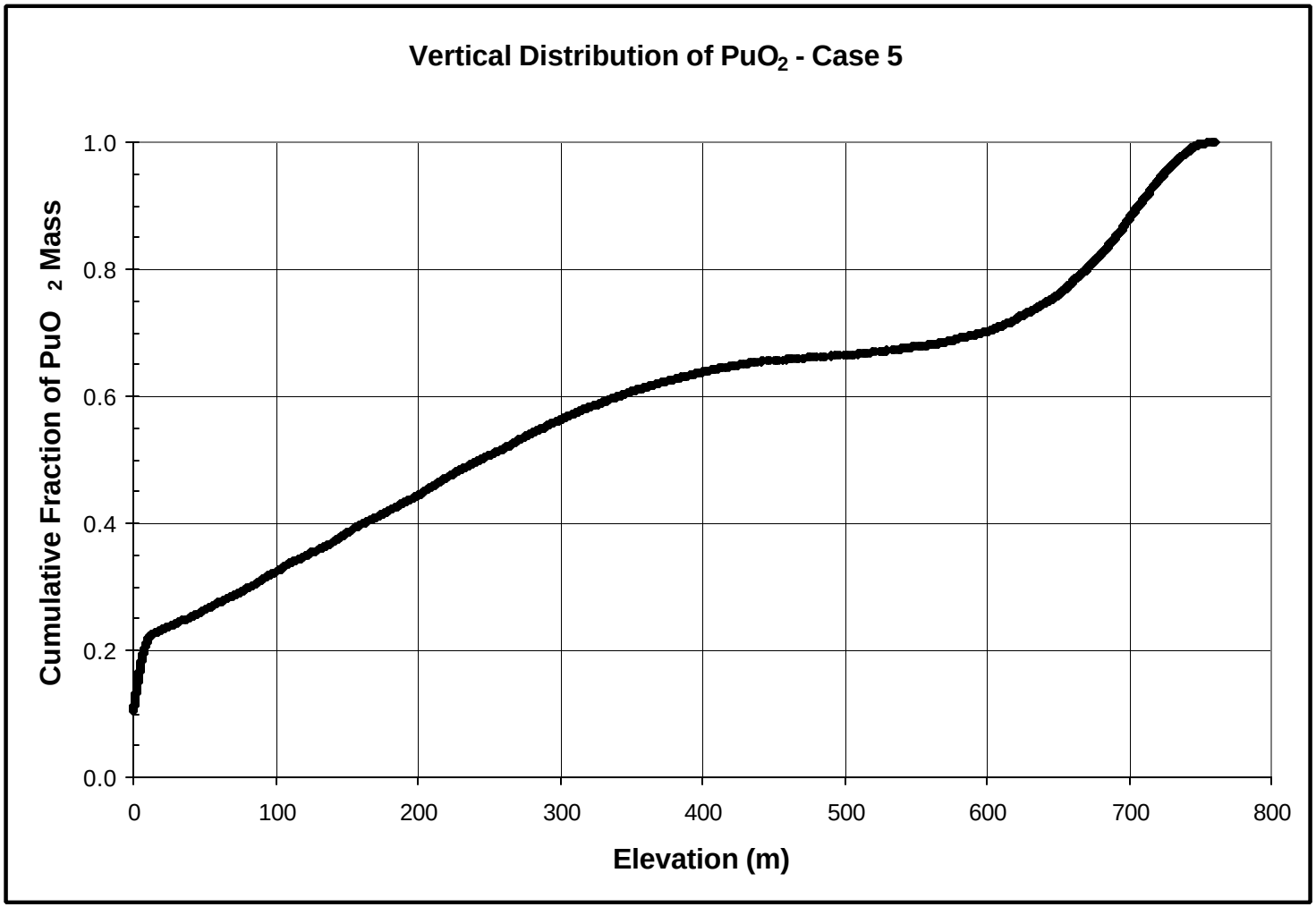

Figure 6.10 Case 5 - Vertical Distribution of PuO_2 Mass in Plume

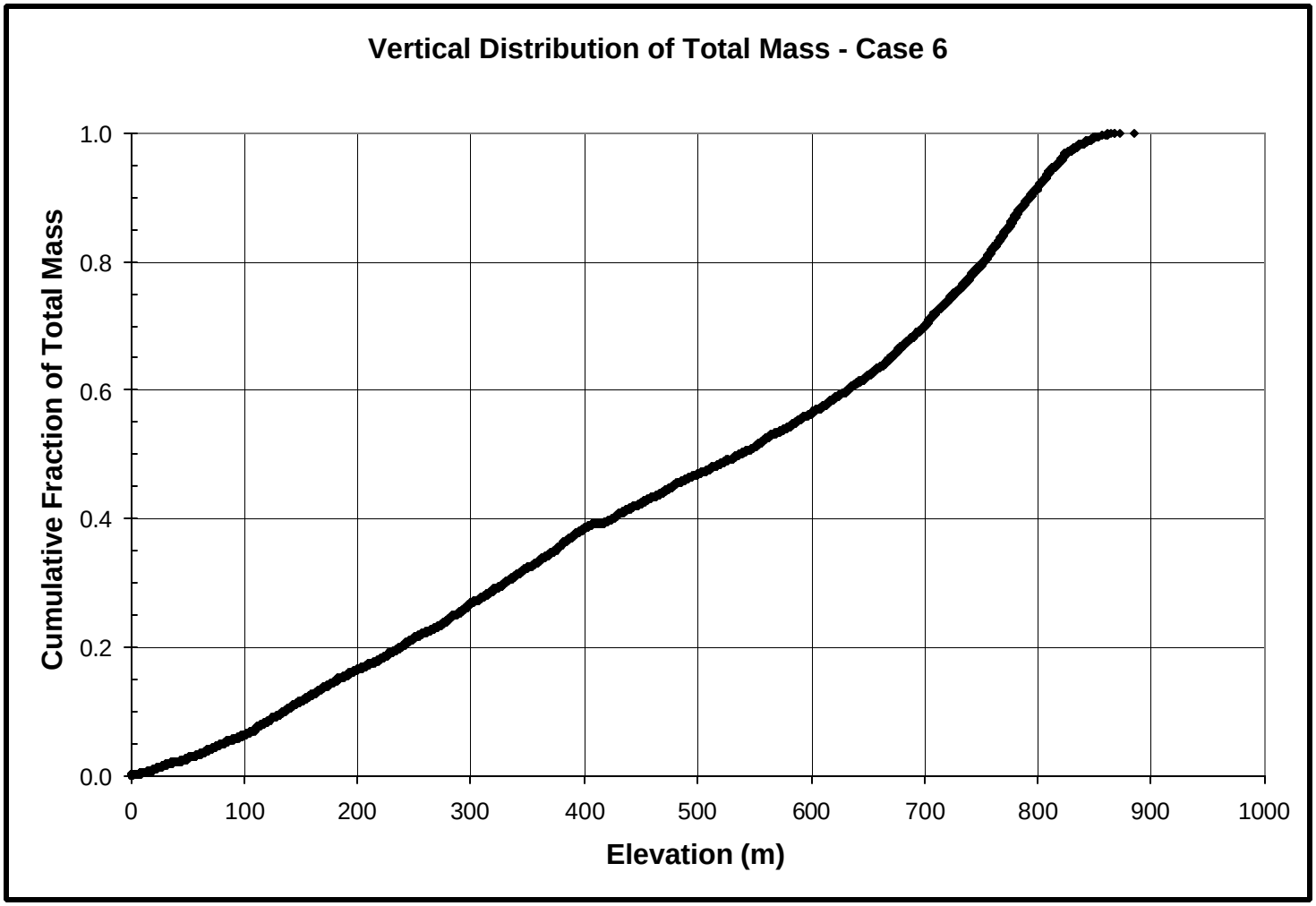

Figure 6.11 Case 6 - Vertical Distribution of Total Mass in Plume

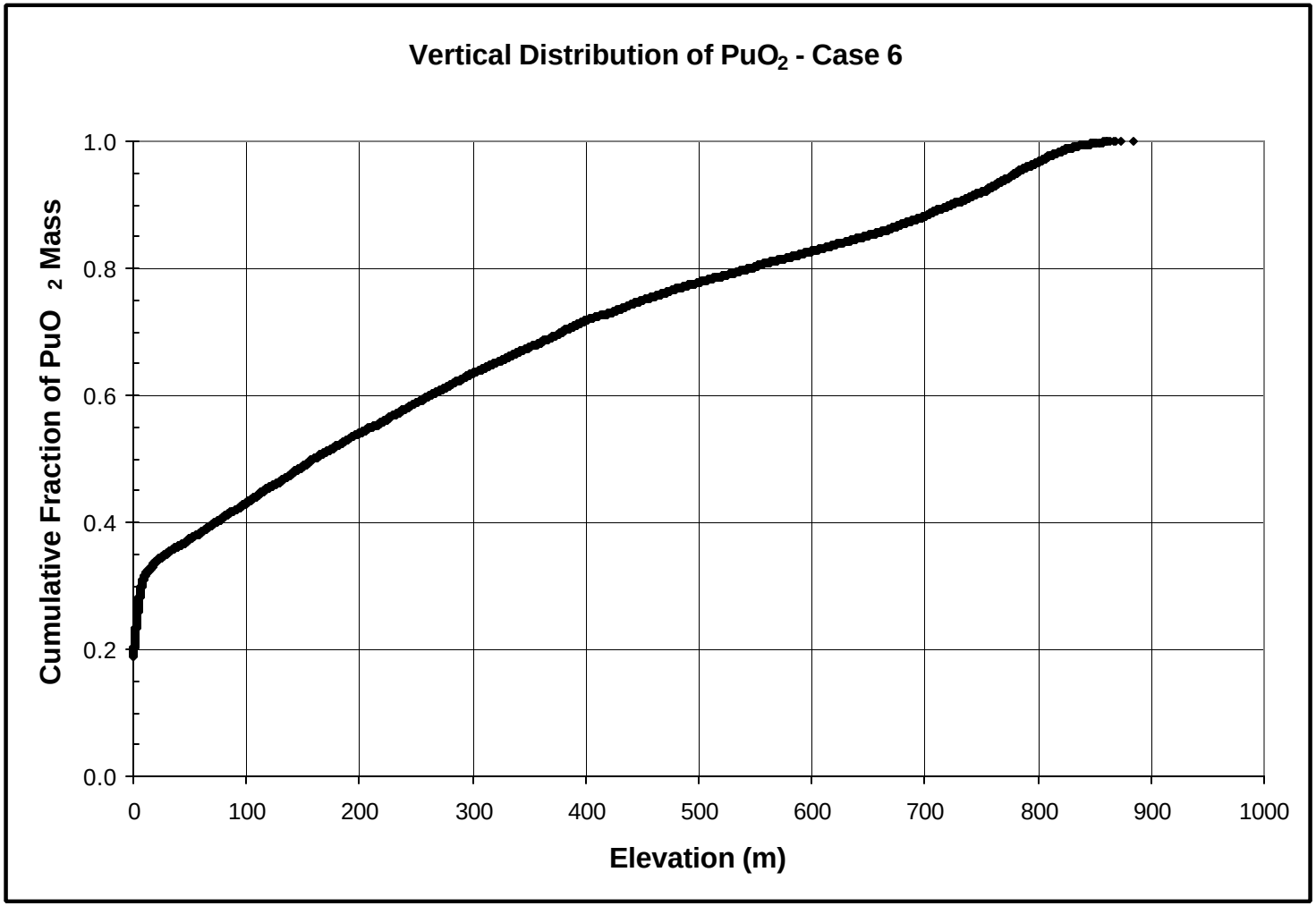

Figure 6.12 Case 6 - Vertical Distribution of PuO_2 Mass in Plume

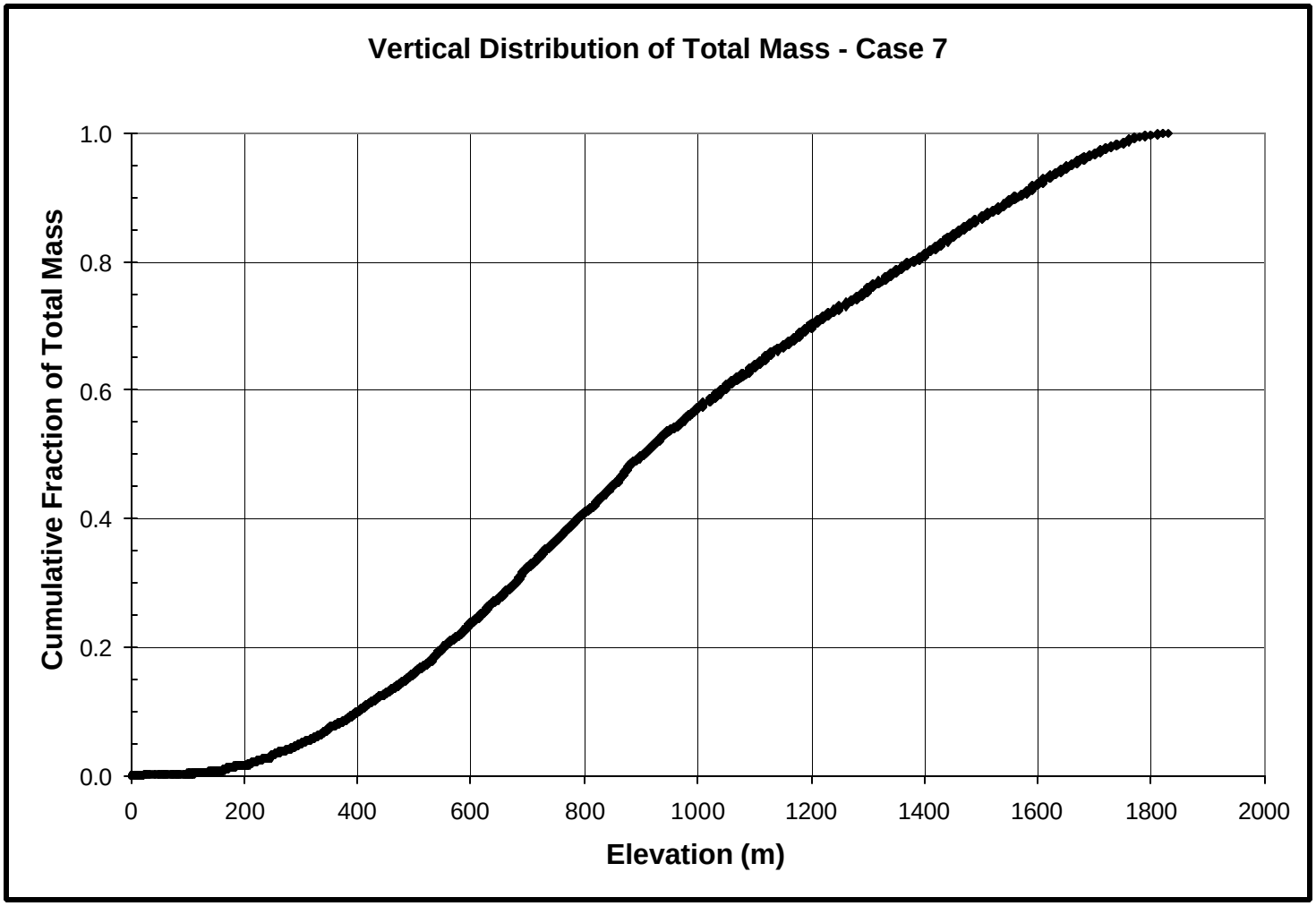

Figure 6.13 Case 7 - Vertical Distribution of Total Mass in Plume

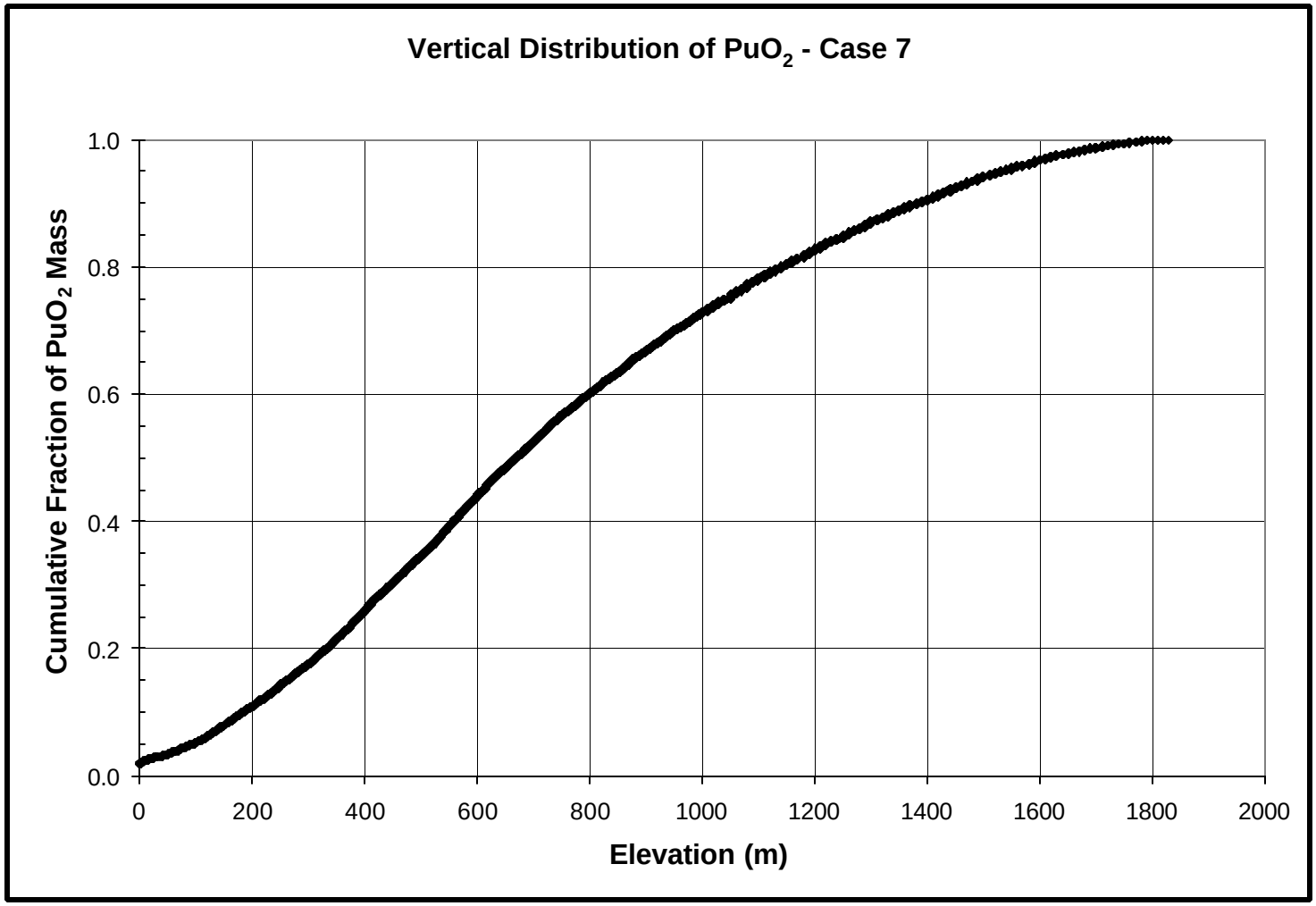

Figure 6.14 Case 7 - Vertical Distribution of PuO_2 Mass in Plume

Figure 6.15 illustrates for the H/D ratios, the amount of total and PuO_2 mass in the plume stem (the PuO_2 mass is provided both with and without the ground deposited PuO_2 mass). Typically for the lowest H/D ratios, there is more mass in the lower regions of the cloud. The stem mass then decreases until the H/D ratios attain values of about 5. Above the H/D ratios of about 5, the stem mass then begins to slowly increase again as H/D increases. For the data presented here, it appears that for the total plume mass, the moderate to high H/D ratios (>3) agree with the classical stem and cap model (i.e. less mass in the lower regions of the cloud). For the PuO_2 plume mass, the moderate H/D ratios (~3-10) agree with the classical model; whereas, for higher values of H/D, the higher density PuO_2 particles tend to be located in the lower portions of the plume. In summary, for very low H/D ratios (~1-2), the bulk of plume mass (both total and PuO_2) does not penetrate the inversion layer and the mass distribution is fairly uniform. For moderate H/D ratios (~3-10), the bulk of the plume mass (both total and PuO_2) penetrates the inversion layer and is located in the upper portions of the plume, i.e., in the cap. For high H/D ratios (>10), the lighter particles (represented by the total plume mass) behave like they do for moderate H/D ratios, exhibiting most of the plume mass in the plume cap. However, for the heavier PuO_2particles, even though the plume energy is sufficient to loft most of the mass above the inversion layer, most of the particles are too dense to be contained in the highest elevations of the plume, and the mass distribution can be approximated as uniform. Another point to note is that in some cases substantial amounts of the heavy PuO_2 particles are predicted to deposit on the ground (exhibited for cases 1, 4, 5 and 6 - typically the low and high range H/D values).

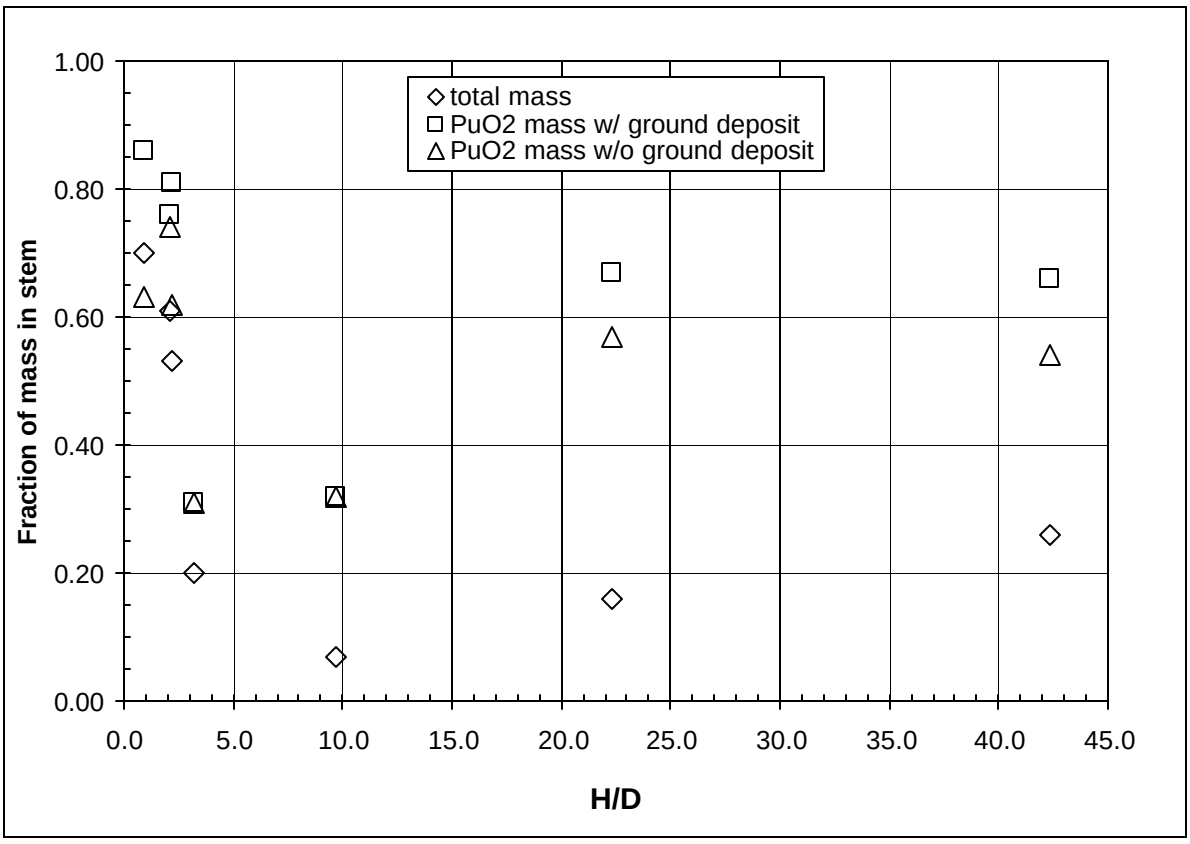

Figure 6.15 H/D Influence on Amount of Plume Mass in Stem

7.0 Conclusions and Recommendations

The results of this study suggest two basic models of the mass distribution in the cap and stem in a lofted plume. The first is the classical model of a cap and stem, for which the percentage of the plume mass contained in the cap and stem is about 80% and 20%, respectively. The second is a uniform distribution of the mass throughout the plume. Because of particle density differences, the mass distribution models indicated for the total plume mass configuration are different from the PuO_2 particle mass configuration (for this study, less than 0.1% of the plume mass is PuO_2).

For the total fireball plume mass in this study, the classical model of a cap and stem is indicated for cases 1, 2, 3, and 5, where the fraction of mass in the stem is between about 0.05 to 0.3. Cases 2 and 5 are low energy scenarios (7.1×10^9 J) in which the mixing layer depths are at 34 m and the Pasquill classification is moderately stable. Cases 1 and 3 are high energy scenarios (4.98×10^{11} J) with mixing layer depths at 145 m and 485 m with slightly stable and neutral stability classes, respectively. A measure of the mixing layer penetration by the plume is indicated by the ratio H/D, where H is the cloud height, and D is the mixing layer depth. Cases 2 and 3 exhibit a moderate H/D ratio (between 3-10), whereas, cases 1 and 5 exhibit a high H/D ratio (>10). In cases 4, 6 and 7, the mixing layer is high relative to the energy of the cloud, resulting in the fairly uniform distribution of the total plume mass across the height of the plume. Case 4 and 6 are low energy scenarios with mixing layer depths of 884 m and 406 m respectively, whereas case 7 is a high energy scenario with a mixing layer depth of 884 m. These three cases all have a neutral to slightly stable Pasquill classification, and perhaps of more significance, these cases have simulated plume heights that are greater than the mixing depth layer by less than a factor of three, i.e., they exhibit a low H/D ratio (< 3).

The classical model for the PuO_2 mass distribution in the fireball plume is also indicated for cases 2 and 3, where the fraction of mass in the stem is about 0.3. However, the PuO_2 mass in the remaining cases (1, 4, 5, 6 and 7) is more uniformly distributed throughout the cloud. Also, in cases 1, 4, 5 and 6, substantial amounts of the heavy PuO_2 particles are predicted to deposit on the ground. Hence, this study indicates that for heavier particles, the classical cap and stem model is approximated only when the H/D ratio is moderate; that is, when the plume height exceeds the mixing layer by more than a factor of two but is still within an order of magnitude. The approximation does not hold when either the plume energy is insufficient to loft the plume to a height at least twice that of the mixing layer or the plume energy is substantial enough to loft the plume to a height exceeding that of the mixing layer by more than an order of magnitude. The results for the PuO_2 mass distribution for all cases indicate that the consideration of particle size and density distribution is very important to the determination of the cap and stem model quantification.

In the Cassini FSAR radiological consequence analysis as implemented in the SPARRC module, the explosively lofted plume is assumed to consist of a stem and cap portion, with the stem column height calculated as described in Section 5.2 of this report. For the SPARRC module, the consequence analyst specifies the fraction of the airborne mass that is contained in the stem, and the balance of the mass is then assumed to be in the cap. In the variability-only analysis that was performed for the Cassini

Mission FSAR, the fraction of plume mass that was assumed to be in the plume stem was 0.2; for the uncertainty analysis, the distribution of mass in the stem ranged from 0.03 to 0.60. As noted in Section 6.2 of this report, for total plume mass, the FSAR uncertainty analysis is in good agreement with the range of values from this study for total plume mass. However, for the consequence analysis, it is the PuO_2 mass in the plume that is of interest since it is material in the plume that provides dose.

Table 7.1 provides the distribution of values used as input in the Cassini FSAR for the fraction of PuO_2 mass in the plume that is contained in the stem. Also provided in Table 7.1 are suggested updated distributions formulated in light of the information obtained from this study. The suggested updated distributions are provided in terms of two specifications:

1. without a dependence on the H/D ratio, and
2. for three ranges of H/D ratios (H/D < 3, between 3-10, or > 10)

The second option is preferred if the H/D information is available and the implementation of the distributions for the three ranges is possible. If the second option is implemented and if it is possible to specify that some of the stem plume mass be deposited on the ground, then a further adjustment of data is suggested for the first and third H/D ranges. For example, suppose a ground deposit fraction is chosen to be 0.1, then the distribution for H/D < 3 would range from 0.1 to 0.8 and the distribution for H/D > 10 would range from 0.05 to 0.65.

Table 7.1 Distributions for the Fraction of PuO_2 Mass Contained in the Stem

Percentiles	Fraction of PuO_2 Mass in Stem				
	Cassini FSAR distribution	Suggested Updated Distributions			
		no H/D dependency	H/D < 3	3 < H/D < 10	H/D > 10
0th	0.03	0.05	0.2	0.05	0.15
5th	0.1	0.2	0.3	0.1	0.3
50th	0.2	0.6	0.7	0.2	0.4
95th	0.5	0.8	0.8	0.3	0.6
100th	0.6	0.9	0.9	0.5	0.75

In summary, this study indicates that consideration of the density of particles in a lofted plume is important in determining the distribution of mass within the plume. Compared to plumes with lighter particles, plumes with particles of higher density are predicted to accumulate more mass in lower elevations of the plume (a significant amount of the higher density particles may even be deposited on the ground). This study also indicates that the energy of the release relative to the mixing layer depth impacts the vertical mass distribution in a lofted plume. When the energy is sufficient to both penetrate the inversion layer and still loft the plume to elevations that are between about three and ten times the mixing layer depth, then the classical cap and stem approximation is deemed to be adequate. If the energy is more or less than sufficient, then it is better to assume a more uniform vertical distribution of

the mass in the plume.

While this study is limited in its scope, it has provided some important insights for particle behavior within lofted plumes. It has also raised some questions that can be related to possible future work in this area. Some proposed future work includes:

1. Inclusion of more weather days and times to provide a larger sample of weather, mixing layer height and plume lofting energy combinations. While the variation in these parameters across the cases in this study was not insignificant, the potential parameter space to be covered is very large. More statistical analysis could be performed if there were a larger number of cases included; for example, the validity of the H/D ratio correlation postulated in this study could be investigated.
2. Inclusion of variation of other parameters, such as in the fireball source term analysis.
3. Investigation of the sensitivity of the mass distribution to particle size.
4. Further investigation of the sensitivity of the mass distribution to particle density.

This page intentionally left blank.

8.0 References

[Boughton, 1992] Boughton, B. A. and J. M. DeLaurentis, "Description and Validation of ERAD: An Atmospheric Dispersion Model for High Explosive Detonations," SAND92-2069, Sandia National Laboratories, Albuquerque, NM, October 1992.

[Chang, 1996] Chang, C. (LMC), private communication (memo fax to J. Gregory, SNL), September 4, 1996.

[Deane, 1996] Deane, N. (LMC), private communication (e-mail to J. Gregory, SNL), September 11, 1996.

[Dobranich, 1997] Dobranich, et al., "The Fireball Integrated Code Package," SAND97-1585, Sandia National Laboratories, Albuquerque, NM, July 1997.

[LMC, 1996] "GPHS-RTGs in Support of the Cassini Mission, Final Safety Analysis Report (FSAR)," CDRL C.3, Contract No. DE-AC03-91SF18852, Lockheed Martin Missiles & Space, Philadelphia, PA, December 1996.

[McBride, 1989] McBride, B., "CET89 – Chemical Equilibrium with Transport Properties, 1989," COSMIC Program # LEW-15113, Lewis Research Center, Cleveland, OH, 1989.

Distribution

External Distribution

5 Nelson Dean
Lockheed Martin Missiles & Space
2770 De La Cruz Blvd.
Santa Cruz, CA 95050

1 Chuong Ha
Lockheed Martin Missiles & Space
2770 De La Cruz Blvd.
Santa Cruz, CA 95050

1 Larry DeFillipo
Lockheed Martin Missiles & Space
Room U8620, Building 100
P.O. Box 8555
Philadelphia, PA 19101

1 Frank Kampas
Lockheed Martin Missiles & Space
Room U8620, Building 100
P.O. Box 8555
Philadelphia, PA 19101

1 Jack Chan
Lockheed Martin Missiles & Space
Room U8620, Building 100
P.O. Box 8555
Philadelphia, PA 19101

1 Hank Firstenberg
Tetra Tech NUS
Suite 400
910 Clopper Rd.
Gaithersburg, MD 20878

1 Bart Bartrum
Tetra Tech NUS
Suite 400
910 Clopper Rd.
Gaithersburg, MD 20878

1 Earl Wahlquist
U.S. Department of Energy
Germantown Building, NE-50
19901 Germantown Road
Germantown, MD 20874

1 Rich Furlong
U.S. Department of Energy
Germantown Building, NE-50
19901 Germantown Road
Germantown, MD 20874

1 Art Mehner
U.S. Department of Energy
Germantown Building, NE-50
19901 Germantown Road
Germantown, MD 20874

1 Don Owings
U.S. Department of Energy
Germantown Building, NE-50
19901 Germantown Road
Germantown, MD 20874

1 Lyle Rutger
U.S. Department of Energy
Germantown Building, NE-50
19901 Germantown Road
Germantown, MD 20874

1 Jack Wheeler
U.S. Department of Energy
Germantown Building, NE-50
19901 Germantown Road
Germantown, MD 20874

1 F. Eric Haskin

ERI Consulting
901 Brazos Place SE
Albuquerque, NM 87123

1 Michael Frank
Safety Factor Associates
4401 Manchester Ave., Suite 106
Encinitas, CA 92024

1 Capt. Ed Jakes, USAF
HQ AFSC/SEWE
9700 Avenue G
Bldg. 2499, Suite 120
Kirtland AFB, NM 87117-5670

1 Gareth Parry
U.S. Nuclear Regulatory Commission
NRR/DSSA
11555 Rockville Pike, MS O-10A1
Rockville, MD 20852-2738

1 Nathan Siu
Probabilistic Risk Analysis Branch
MS 10E50
U.S. Nuclear Regulatory Commission
Washington, DC 20555-0001

1 Yale Chang, 1E-260
The Johns Hopkins University
Applied Physics Laboratory
11100 Johns Hopkins Rd.
Laurel, MD 20723-6099

1 Orbital Sciences Corp.
Attn: Cassini Project Office
2031 Century Blvd.
Germantown, MD 20874-1110

1 Dr. Louis Goossens
Delft University of Technology
TBM/VK
P.O. Box 5050
NL-2600 GB Delft
The Netherlands

1 Berndt Kraan
Delft University of Technology
Mekelweg 4
Room 5.050
2627 CA Delft
The Netherlands

Sandia Distribution

1	MS 0405	12333	Todd Jones
1	MS 0428	12300	David Carlson
1	MS 0428	12301	William McCulloch
1	MS 0449	6514	Donald Gallup
1	MS 0492	12332	Kevin Maloney
1	MS 0736	6400	Thomas Blejwas
1	MS 0742	6401	John Guth
1	MS 0744	6420	Dennis. Berry

1	MS 0747	6410	Allen Camp
1	MS 0747	6410	Roger Cox
5	MS 0747	6410	Vince Dandini
1	MS 0747	6410	Felicia Duran
1	MS 0747	6410	Jeff LaChance
1	MS 0747	6410	Teresa Sype
1	MS 0747	6410	Gregory Wyss
1	MS 0748	6413	David Robinson
1	MS 0748	6413	Bob Waters
1	MS 0748	6413	Tim Wheeler
1	MS 0748	6413	Donnie Whitehead
10	MS 0767	5817	Frederick Harper
1	MS 0767	5817	Bruce Boughton
1	MS 0828	9133	Martin Pilch
1	MS 0828	9133	William Oberkampf
1	MS 0829	12323	Floyd Spencer
1	MS 0830	12335	Kathleen V. Diegert
1	MS 0836	9117	Dean Dobranich
10	MS 0977	6524	Julie Gregory
1	MS 0977	6524	Bill Richard
1	MS 1136	6424	Paul Pickard
1	MS 1137	6534	Sharon Deland
1	MS 1176	15312	Dennis Anderson
1	MS 1176	15312	Robert Cranwell
1	MS 1176	15312	Laura Swiler
1	MS 0918	8945-1	Central Technical Files
2	MS 0899	9616	Technical Library
1	MS 0612	9612	Review and Approval Desk for DOE/OSTI